iScience

CellPress
OPEN ACCESS

Article

Profiling ovarian cancer tumor and microenvironment during disease progression for cell-based immunotherapy design

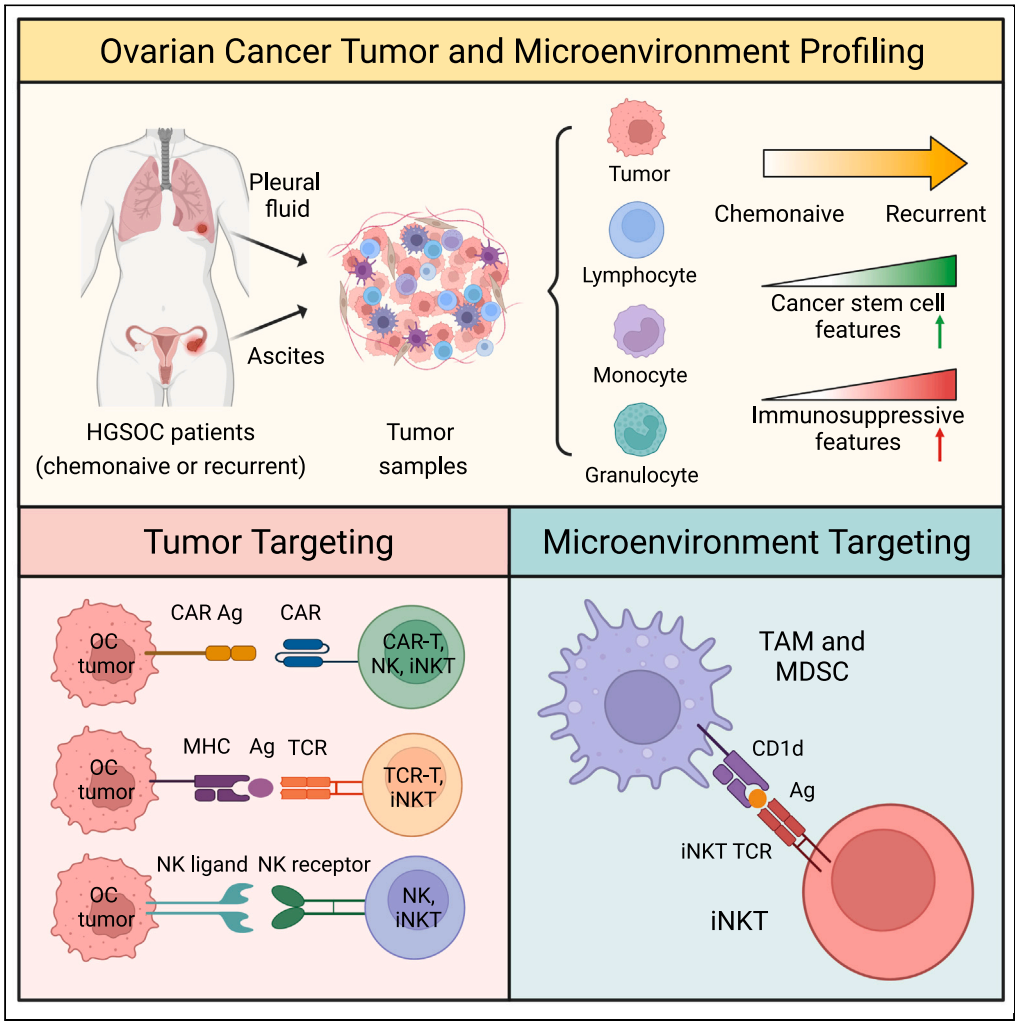

Yan-Ruide Li, Christopher J. Ochoa, Yichen Zhu, ..., Jin J. Zhou, Sanaz Memarzadeh, Lili Yang

smemarzadeh@mednet.ucla.edu (S.M.)
liliyang@ucla.edu (L.Y.)

Highlights

Profile a set of OC patient samples spanning chemonaive and recurrent diseases

Recurrent OC tumor cells are CSC-enriched and vulnerable to TCR/NKR/CAR killing

Recurrent OC TME abounds with TAMs and MDSCs expressing a targetable biomarker CD1d

Provide a roadmap to design cell-based immunotherapy strategies for OC

Li et al., iScience 26, 107952
October 20, 2023
https://doi.org/10.1016/j.isci.2023.107952

iScience

CellPress
OPEN ACCESS

Article

Profiling ovarian cancer tumor and microenvironment during disease progression for cell-based immunotherapy design

Yan-Ruide Li,[1,10] Christopher J. Ochoa,[2,3,4,10] Yichen Zhu,[1] Adam Kramer,[1] Matthew Wilson,[1] Ying Fang,[1] Yuning Chen,[1] Tanya Singh,[2,4,5] Gabriella Di Bernardo,[2,4,5] Enbo Zhu,[1] Derek Lee,[1] Neda A. Moatamed,[6] Joanne Bando,[7] Jin J. Zhou,[8] Sanaz Memarzadeh,[2,3,4,5,9,*] and Lili Yang[1,3,4,5,11,*]

SUMMARY

Ovarian cancer (OC) is highly lethal due to late detection and frequent recurrence. Initial treatments, comprising surgery and chemotherapy, lead to disease remission but are invariably associated with subsequent relapse. The identification of novel therapies and an improved understanding of the molecular and cellular characteristics of OC are urgently needed. Here, we conducted a comprehensive analysis of primary tumor cells and their microenvironment from 16 chemonaive and 10 recurrent OC patient samples. Profiling OC tumor biomarkers allowed for the identification of potential molecular targets for developing immunotherapies, while profiling the microenvironment yielded insights into its cellular composition and property changes between chemonaive and recurrent samples. Notably, we identified CD1d as a biomarker of the OC microenvironment and demonstrated its targeting by invariant natural killer T (iNKT) cells. Overall, our study presents a comprehensive immuno-profiling of OC tumor and microenvironment during disease progression, guiding the development of immunotherapies for OC treatment, especially for recurrent disease.

INTRODUCTION

Ovarian cancer (OC) is the deadliest gynecologic disease in the United States and the second in the world.[1–3] Contributing to this lethality, OC is often diagnosed at late stages, in part, due to the non-specific symptoms associated with its development and the lack of effective screening methods.[1,4–6] As a result, the majority of patients present with disease that has spread beyond the pelvic region.[7] Upon diagnosis, the typical course of treatment for patients consists of a combinatorial approach of surgical removal and chemotherapy administration.[8,9] In the case of OC, the most common chemotherapy administered is some forms of platinum-based therapy, such as carboplatin or cisplatin, in conjunction with a taxane, such as paclitaxel.[8–11] Although most patients show a positive response to initial treatment resulting in a significant reduction in tumor burden, the majority of patients experience OC tumor growth relapse, leading to the development of a more aggressive disease.[12] One reason is the development of a resistance to platinum-based therapies, also known as platinum resistance.[7,13] Hence, effective treatment of platinum-resistant, recurrent disease remains an unmet clinical need in OC.

Immunotherapies emerge as an attractive treatment option for patients with OC, including the use of immunomodulators, such as checkpoint inhibitors and monoclonal antibodies, as well as immune cell-based products, such as chimeric antigen receptor (CAR)-engineered T (CAR-T) cells, T cell receptor (TCR)-engineered T cells, and natural killer (NK) cells.[14–17] Cell-based immunotherapy (CBI) in OC is currently in its early phase of development. Several clinical trials are presently underway to assess the safety and therapeutic potential of various CBIs that target diverse tumor antigens in OC, including mesothelin (NCT01583686) and NY-ESO-1 (NCT01567891). However, there are several significant challenges: the heterogeneity in tumor cells and their antigen expression, the presence of cancer stem cells (CSCs) that are therapy-resistant and immuno-evasive, and an unfavorable tumor microenvironment (TME) comprising immunosuppressive cells like regulatory

[1]Department of Microbiology, Immunology & Molecular Genetics, University of California, Los Angeles, Los Angeles, CA 90095, USA
[2]Department of Obstetrics and Gynecology, David Geffen School of Medicine, University of California Los Angeles, Los Angeles, CA 90095, USA
[3]Molecular Biology Institute, University of California, Los Angeles, Los Angeles, CA 90095, USA
[4]Eli and Edythe Broad Center of Regenerative Medicine and Stem Cell Research, University of California, Los Angeles, Los Angeles, CA 90095, USA
[5]Jonsson Comprehensive Cancer Center, David Geffen School of Medicine, University of California, Los Angeles, Los Angeles, CA 90095, USA
[6]Department of Pathology and Laboratory Medicine, David Geffen School of Medicine, University of California, Los Angeles, Los Angeles, CA 90095, USA
[7]Department of Medicine, Division of Pulmonary and Critical Care, University of California, Los Angeles, Los Angeles, CA 90095, USA
[8]Department of Biostatistics, Fielding School of Public Health, University of California, Los Angeles, Los Angeles, CA 90095, USA
[9]The VA Greater Los Angeles Healthcare System, Los Angeles, CA 90073, USA
[10]These authors contributed equally
[11]Lead contact
*Correspondence: smemarzadeh@mednet.ucla.edu (S.M.), liliyang@ucla.edu (L.Y.)
https://doi.org/10.1016/j.isci.2023.107952

T cells, tumor-associated macrophages (TAMs), and myeloid-derived suppressive cells (MDSCs).[14,18–23] CSCs are cancer cells with stem-like properties such as multi-differentiation, chemoresistance, metastasis, and tumor progression.[19,24–31] It is noteworthy that in OC there is a reciprocal interaction between CSCs and TAMs/MDSCs. Specifically, CSCs secrete certain factors that induce the polarization and persistence of TAMs/MDSCs into an immunosuppressive state,[32–35] and TAMs/MDSCs play a role in the formation of the tumor niche that supports CSCs.[19,26,27,32–35] In addition, immunosuppressive TAMs and MDSCs are considered major hurdles for many immunotherapies, including immune checkpoint blockade and adoptive CAR-T cell therapies.[22,23,36–40] Therefore, the development of novel CBIs and combination therapies that can simultaneously target both the OC cancer cells and TME may hold great promise as a next-generation approach in treating this aggressive malignancy.

One major roadblock in designing an effective CBI for OC is the lack of a comprehensive immune target profile for OC that details the immune target biomarkers on OC tumor cells and in OC TME during disease progression. Here, we report a study addressing this critical need. We collected a total of 26 primary OC patient samples spanning chemonaive and recurrent disease states, profiled the OC tumor cells and TME using flow cytometry (for tumor antigens, CSC biomarkers, and TME cell compositions and properties), and evaluated various CBIs against these primary OC patient samples (for TCR-, CAR-, and NKR-directed CBIs). Our study generated a comprehensive immune target profile for OC that can valuably guide the development of next-generation CBIs for OC, especially for treating disease recurrence. Notably, we identified CD1d as a biomarker of the OC TME and highlighted the therapeutic potential of invariant natural killer T (iNKT) cell therapy, which we show is capable of targeting both OC tumor cells and the TME through multiple molecular mechanisms.

RESULTS

Collecting primary OC patient samples

To profile OC patient samples and develop corresponding cell-based therapy, a total of 26 primary OC patient samples were collected from ascites or pleural fluid sources (Table 1). We focused our analysis on ascites and pleural fluid samples due to the aggressive nature of OC that results in the presence of these fluid buildups.[41,42] Ascitic tumor cells are shed from the primary ovarian tumor and can be thought of as portals to seed distant metastases, while pleural fluid tumor cells are the results of metastatic OC to the lung.[41,42] Therefore, utilizing patient samples derived from these two sources will allow us to focus on the most aggressive and metastatic-like nature of OCs. All patients were diagnosed with high-grade serous ovarian cancer (HGSOC), with one patient presenting with sarcomatous (sample #6), one with endometrioid (sample #7), and one with clear cell carcinoma (sample #12) elements as well. These OC patient samples were divided into two subgroups based on chemotherapy status: chemonaive (samples #1–13, 21C, 22C, and 23C) and recurrent (samples #14–20, 21R, 22R, and 23R). Notably, three matched samples were collected from the same patient before and after chemotherapy (samples #21–23). Additionally, based on platinum sensitivity, the OC patient samples were divided into two subgroups: sensitive and resistant samples (Table 1). All 26 primary OC samples were included in subsequent experiments.

Profiling OC tumor and developing cell-based immunotherapies

In the hopes of determining the effectiveness of current cell-based immunotherapies in treating OC, we profiled the 26 OC sample-derived tumor cells using multi-panel flow cytometry to assess the surface expression of common immunotherapeutic targets (Figures 1A, 1B, and S1A–S1C). These targets included CAR antigens (i.e., mesothelin/MSLN and MUC16), TCR antigens (i.e., New York esophageal squamous cell carcinoma 1/NY-ESO-1), and NK activating ligands (i.e., ULBP-1, ULBP-2/5/6, MICA/B, CD112, and CD155)[14,43–48] (Figures 1C and 1D). Notably, while only a selection of antigens were tested in this study, other OC antigens such as HER2, FRα, and GPC3 could also be potential subjects of investigation.[49–51] The ESO TCR target, NY-ESO-1, exhibited minimal expression and heterogeneous expression patterns across our study cohort (Figures 1C and 1D). On the other hand, CAR targets, particularly MSLN, demonstrated relatively higher expression in certain patients but also exhibited heterogeneity in their expression levels (Figures 1C and 1D). NK ligands ULBP-1 and ULBP-2/5/6 were near absent, while other NK ligands MICA/B, CD112, and CD155 showed almost universally expression across our patient cohort, which could open the door for NK receptor (NKR)-mediated cell killing (Figures 1C and 1D). It is noteworthy that we observed minimal variation in the expression of these tumor antigens among the three pairs of matched OC patients, suggesting that these antigens exhibit conserved expression levels following chemotherapy (Figures 1C and 1D). Given the observed overall heterogeneous surface expression of immunotherapeutic targets across the 26 OC sample cohort, we set out to test the effectiveness of these three different targeting systems using *in vitro* tumor cell killing assays by co-culturing the OC patient tumor cells with specific therapeutic cells.

Using MSLN-targeting CAR-engineered T (MCAR-T) cells, we observed that OC patient tumor cells with high surface expression of MSLN were more effectively targeted by the MCAR-T cells, whereas tumor cells with medium and low surface expression of MSLN were less and not affected by the MCAR-T cells, correspondingly (Figures 1E, 1F, and S1D). We noticed a similar concordance between surface expression of NY-ESO-1 and the ability of ESO TCR-engineered T (ESO-T) cells to kill tumor cells (Figures 1G and 1H). The elevated expression levels of NK cell activating ligands on OC tumor cells facilitate the recognition and targeting of these tumor cells by NK cells (Figure S1E).[15] This was verified by the effective targeting of OC patient tumor cells with peripheral blood mononuclear cell (PBMC)-derived NK cells (Figure 1I). These findings suggest that different CBIs could be developed to target OC tumor cells with distinct antigen expression profiles.

Here we propose a possible stratification strategy to optimize treatment approaches based on distinct OC tumor characteristics. Firstly, tumor cells showing positivity for CAR antigens but negativity for ESO TCR antigens (e.g., MSLN^{high}NY-ESO-1^{low}) could be prioritized for CAR-T cell therapy. Conversely, tumors expressing ESO TCR antigens while lacking CAR antigens (e.g., MSLN^{low}MUC16^{low}NY-ESO-1^{high}) may benefit more from ESO-T cell therapy. In cases where both CAR and ESO TCR antigens are present on OC tumor cells (e.g.,

Table 1. Clinical ovarian cancer (OC) patient samples

	Sample ID	Diagnosis	Type	Stage	Treatment Status	Platinum Sensitivity
CHEMONAIVE (pre-therapy) n = 13	1	HGSOC	Ascites	3C	Chemonaive	Sensitive
	2	HGSOC	Ascites	3C	Chemonaive	Sensitive
	3	HGSOC	Ascites	3C	Chemonaive	Sensitive
	4	HGSOC	Ascites	3C	Chemonaive	Sensitive
	5	HGSOC	Ascites	3C	Chemonaive	Sensitive
	6	HGSOC (80%) with sarcomatous elements (20%)	Ascites	2B	Chemonaive	Sensitive
	7	HGSOC (90%), endometrioid (10%)	Ascites	3C	Chemonaive	Sensitive
	8	HGSOC	Ascites	4B	Chemonaive	Resistant
	9	HGSOC	Ascites	4A	Chemonaive	Resistant
	10	HGSOC	Ascites	3C	Chemonaive	Resistant
	11	HGSOC	Pleural Fluid	4B	Chemonaive	Resistant
	12	HGSOC & clear cell carcinoma	Ascites	3C	Chemonaive	Resistant
	13	HGSOC	Ascites	3C	Chemonaive	Resistant
RECURRENT n = 7	14	HGSOC	Ascites	3C	Recurrent	Resistant
	15	HGSOC	Pleural Fluid	3C	Recurrent	Resistant
	16	HGSOC	Pleural Fluid	2A	Recurrent	Resistant
	17	HGSOC	Pleural Fluid	3C	Recurrent	Resistant
	18	HGSOC	Ascites	2A	Recurrent	Sensitive
	19	HGSOC	Pleural Fluid	4A	Recurrent	Resistant
	20	HGSOC	Pleural Fluid	4B	Recurrent	Resistant
MATCHED n = 6	21C	HGSOC	Ascites	3C	Chemonaive	Sensitive
	21R	HGSOC	Pleural Fluid	3C	Recurrent	Resistant
	22C	HGSOC	Ascites	3C	Chemonaive	Sensitive
	22R	HGSOC	Ascites	3C	Recurrent	Resistant
	23C	HGSOC	Ascites	3C	Chemonaive	Resistant
	23R	HGSOC	Ascites	3C	Recurrent	Resistant

MSLN^{high}NY-ESO-1^{high}), a combination therapy involving a cell product expressing both CAR and ESO TCR could be considered. Notably, when tumor cells are negative for both CAR and ESO TCR antigens (e.g., MSLN^{low}MUC16^{low}NY-ESO-1^{low}), the uniform expression of NK ligands on these cells suggests the potential for NK cell therapy. Based on the expression levels of MSLN and NY-ESO-1, the 26 OC samples were classified into four distinct groups (Figures S2A). The effectiveness of tumor cell killing by the corresponding CBIs was verified (Figures S2B), thereby justifying the rationale of the proposed stratification strategy. Collectively, comprehensive screening and profiling of tumor cells offer a promising avenue for the development of tailored and effective cell-based therapies in the context of OC treatment.

While several studies have reported an increase in human leukocyte antigen (HLA) expression in OC cells following chemotherapy treatment,[52–55] our analysis of the 26 OC patient samples did not reflect a difference in HLA expression between chemonaive and recurrent OC cells (Figures S3A and S3B). It is important to note that the extent and mechanism of HLA expression changes may depend on the specific chemotherapy regimen and individual tumor characteristics. Further investigation is warranted to elucidate the complex relationship between chemotherapy and HLA expression in OC.

An additional recent target for current therapies has been tumor cells with an increased stem-like nature, termed cancer stem cells (CSCs).[19,24–31] Previous studies have identified cells with CSC-like characteristics to express markers such as CD24, CD44, CD117, CD133, Nanog, Oct3/4, and SOX2.[26,27,29,31,56–59] Traditional stem cell transcription factors (TFs) Nanog, Oct3/4, and SOX2 have been previously noted as key regulators of stemness, and their aberrant expression in disease states promotes stem-like traits.[60] Therefore, a comprehensive profiling of CSC markers was conducted in our patient cohort to assess the presence of CSC markers in tumor cells derived from chemonaive or recurrent OC patients. In looking at the 3 pairs of OC patient-matched samples, we observed an overall increase in the expression of stem cell TFs in our recurrent samples, compared to the matched chemonaive samples (Figures 1J and S3C). Furthermore, in the entire cohort, a greater proportion of recurrent OC patient samples expressed all three stem cell TFs to a higher degree than the chemonaive OC cohort (Figures 1K, S4A, and S4B). Additionally, the recurrent OC cohort also showed a greater proportion of patients double-positive for various

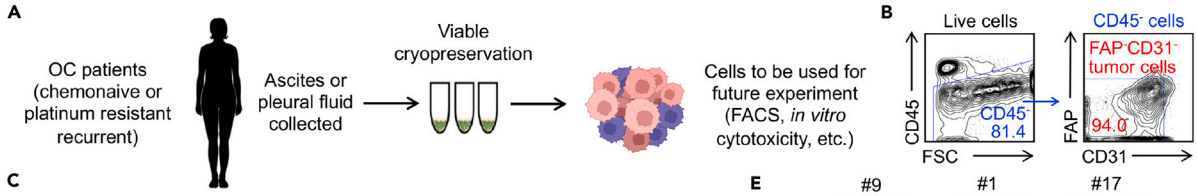

C

Sample ID	Tumor antigens (Ags)							
	CAR Ags		ESO TCR Ag	NK ligands				
	MSLN	MUC16	NY-ESO-1	ULBP-1	ULBP-2/5/6	MICA/B	CD112	CD155
1	++	+	-	+	-	+++++	+++++	++
2	-	-	-	-	++	+	-	+++++
3	++	+	+	-	-	+	+++++	++
4	++	++	-	-	-	-	+++++	+++++
5	+	-	-	+	+	++	++	++
6	-	+	-	+	-	+	+++++	+++
7	+	-	-	-	-	++	+++	++
8	+	-	-	-	-	-	+++	++
9	++++	-	-	+	-	-	+++++	+++
10	-	-	-	-	-	+++	++	-
11	-	-	-	-	-	+++	++	+
12	-	+	++	-	++	++	++++	+
13	-	+	+	-	-	++	+++++	+++
14	-	-	-	-	-	++++	++	+++
15	++++	-	++	-	+	+	-	+
16	-	+	+	-	-	++++	+++++	+++++
17	-	+	+	+	-	+	++	++++
18	+	+	-	-	-	++	++++	+
19	++++	+	-	-	-	+++	+++++	+++
20	+++	+	-	+	-	+++	+++++	+++
21C	++	-	-	-	-	++	+	+
21R	++	-	-	-	-	++	+	+
22C	+	+	-	-	-	-	++++	++
22R	+	+	-	+	-	+	+++++	+
23C	+	-	-	-	-	++	++	-
23R	+	-	-	+	-	++	++++	++

+++++ Expression > 80%
++ Expression 20-40%
++++ Expression 60-80%
+ Expression 5-20%
+++ Expression 40-60%
- Expression < 5%

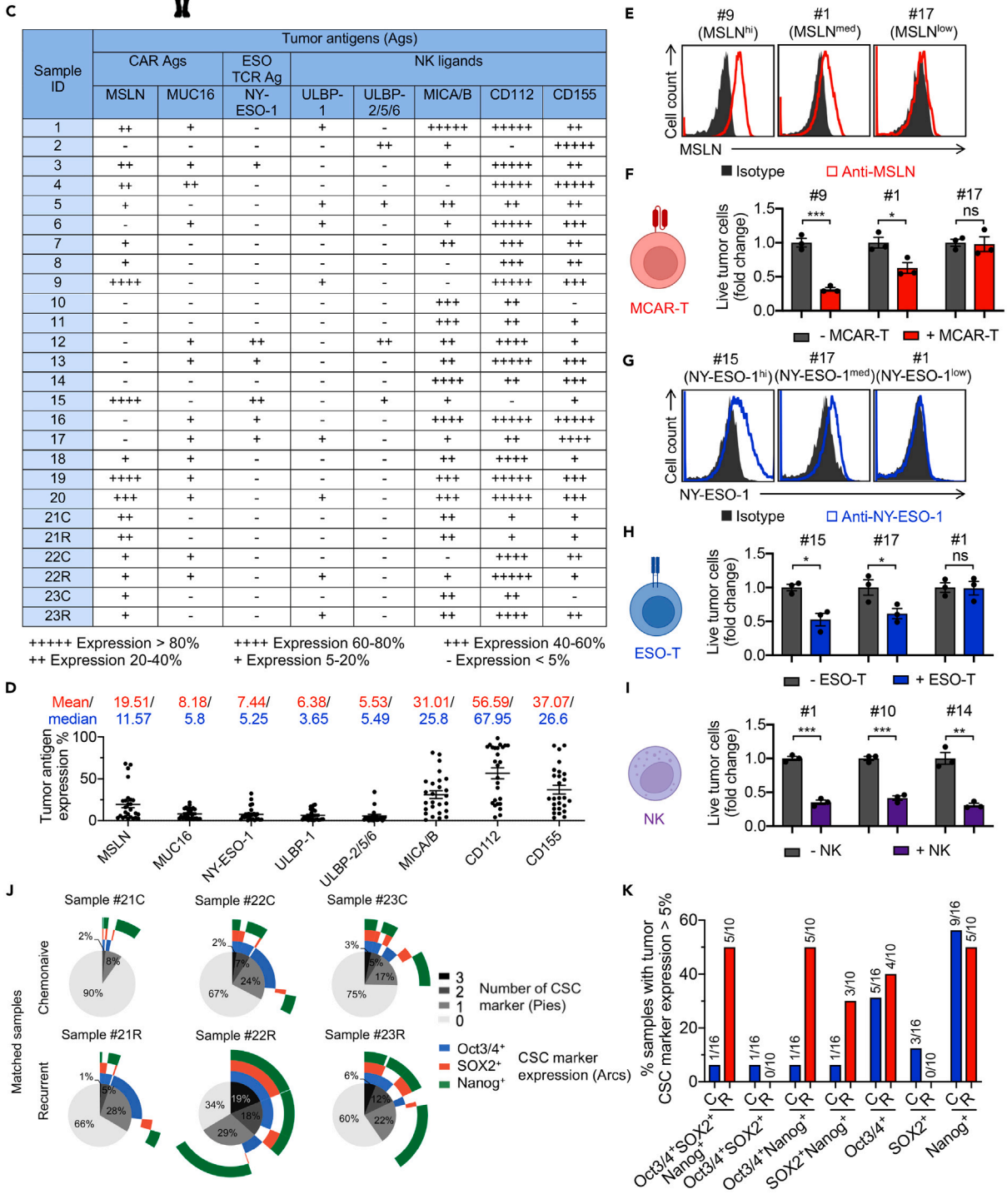

Figure 1. Profile OC tumor cells and evaluate cell-based immunotherapy (CBI) strategies

(A) Experimental design to collect and study tumor and immune cells from primary OC patient samples.

(B) Flow cytometry showing the OC patient sample-derived tumor cells. Tumor cells were identified as non-immune/fibroblast/endothelial (CD45-FAP-CD31$^-$) cells. FAP, fibroblast activation protein.

(C) Table showing the antigen expression level on tumor cells from 26 OC samples. CAR, chimeric antigen receptor; MSLN, mesothelin; MUC16, mucin-16; ESO, esophageal squamous cell carcinoma; NY-ESO-1, New York ESO-1; NK, natural killer cell; MICA/B, MHC class I chain related-proteins A and B; ULBP, UL16 binding protein.

(D) Quantification of tumor antigen expressions from the 26 OC samples.

(E and F) MSLN expression on tumor cells and MSLN-targeting CAR-engineered T (MCAR-T) cell targeting. (E) FACS analyses of MSLN expression on tumor cells from three OC patient samples. MSLN high-, medium-, and low-expressing tumor samples were presented. (F) OC tumor cell killing data by MCAR-T cells at 24 h (E:T = 1:1, n = 3). - MCAR-T, no MCAR-T cells co-cultured with tumor cells. (G-H) NY-ESO-1 expression on tumor cells and ESO TCR-engineered T (ESO-T) cell targeting.

(G) FACS analyses of NY-ESO-1 expression on tumor cells from three OC patient samples. NY-ESO-1 high-, medium-, and low-expressing tumor samples were presented.

(H) OC tumor cell killing data by ESO-T cells at 24 h (E:T = 2:1, n = 3). - ESO-T, no ESO-T cells co-cultured with tumor cells.

(I) OC tumor cell killing data by PBMC-derived NK cells at 24 h (E:T = 5:1, n = 3). - NK, no NK cells co-cultured with tumor cells.

(J and K) FACS analyses of cancer stem cell (CSC) features of tumor cells from 26 OC samples. Transcription factors Oct3/4. SOX2, and Nanog were used as OC CSC markers. (J) SPICE analysis of CSC marker expression from 3 pairs of matched OC samples. Pie charts reflect proportions of indicated tumor cell groups expressing indicated numbers (0–3) of CSC markers. Colored arcs indicate the specific combinations of CSC markers expressed. (K) Summary of OC patient samples categorized based on the expression level of CSC markers. The ratios above the bar represent the number of marker-positive samples versus the total number of samples. Representative of 1 (C, D, J, and K) and >20 (A, B, and E-I) experiments. Data are presented as the mean ± SEM. ns, not significant, *$p < 0.05$, **$p < 0.01$, ***$p < 0.001$, by Student's t test.

combinations of the stem cell TFs, including Oct3/4/Nanog and SOX2/Nanog, compared to the chemonaive OC patient samples (Figure 1K). Although CSC surface markers (CD24, CD44, CD117, and CD133) were similarly analyzed, we did not see a consistent difference within the patient-matched and entire cohort (Figures S4C and S4D).

Deciphering OC TME

Given the limited efficacy of conventional immunotherapeutic approaches in treating OC patients, a significant contributing factor is the impact of the TME on negating treatment effectiveness.[61–63] In light of this, we aim to investigate the cellular composition of our OC patient cohort by thoroughly examining the immune cell populations present within the TME.

Using a multi-panel set of surface markers, we were able to determine the immune cell proportions in TME of the 26 OC patient samples (Figure 2A). A major contributor to the cellular makeup of the TME in the OC cohort was immunosuppressive myeloid cells, such as TAMs and MDSCs (Figure 2A). We investigated the surface expression of different markers associated with M1-like macrophages (i.e., CD86) and M2-like macrophages (i.e., CD163 and CD206)[64–68] and found that the expression of all markers was higher in TAMs compared to other immunosuppressive cells such as MDSCs (Figures 2B and 2C). These findings indicate that TAMs possess more mature and differentiated characteristics when compared to MDSCs, which align with previous research demonstrating that infiltrating MDSCs can differentiate into TAMs and contribute to TAM replenishment via Toll-like receptor (TLR) and cytokine signaling.[69–71] Other immune cells in OC TME were also detected and analyzed including CD4 T, CD8 T, NK, B, and other cells (e.g., neutrophils, eosinophils, and basophils) (Figure 2D).

It is worth noting that of the 26 OC patient samples analyzed, those that were platinum resistant exhibited a greater proportion of TAMs and a significantly higher ratio of CD4/CD8 T cells compared to their platinum-sensitive counterparts. This increase in CD4/CD8 T cell ratio was also seen when comparing chemonaive samples to their respective recurrent counterparts in our patient-matched cohort (Figures 2E–2H). Further investigation and analysis of CD4 and CD8 T cell populations showed that this increased CD4/CD8 proportion was not due to increased CD4 T cells, but rather a decrease in the population of CD8 T cells (Figures 2I and S5A). In light of the reported correlation between the intratumoral accumulation of CD8 T cells and the overall survival of HGSOC patients, the reduction in CD8 T cell numbers within recurrent OC patient samples presents a potential explanation for their tumor relapse and compromised antitumor reactivity.[72–74] In addition, the analysis revealed a lower proportion of B cells in the TME of platinum-resistant patients, while no significant difference was observed for NK cells (Figure 2I).

We also observed significantly elevated levels of the immunosuppressive TAM marker CD206 and major histocompatibility complex (MHC) II molecule HLA-DR on TAMs from recurrent OC patient samples, as compared to their chemonaive state (Figures 2J–2M). Moreover, there was a downregulation of the M1-like macrophage marker CD86 on TAMs from chemonaive samples to recurrent samples in the three matched OC patients (Figures S5B–S5C). The observed upregulation of M2-like TAM markers and downregulation of M1-like macrophage markers suggest enhanced immunosuppressive features of TAMs within the TME of recurrent patients, which may be associated with tumor relapse and poor therapeutic outcomes.[68,75,76] The high expression of HLA-DR could potentially account for the high CD4/CD8 T ratio observed, although further investigation is needed to confirm this (Figures 2G and 2H). Our analysis unveils a heterogeneous cellular composition within the ascites and pleural fluid accumulations frequently observed in OC patients. Notably, these fluid samples contain a significant abundance of immunosuppressive cells, with TAMs constituting an average of approximately 26.8% of CD45$^+$ immune cells across the 26 OC patient samples analyzed (Figure S5D). Therefore, being able to effectively and safely target these immunosuppressive cells seen in OC may prove significant in shifting the balance within the TME to an antitumor state.

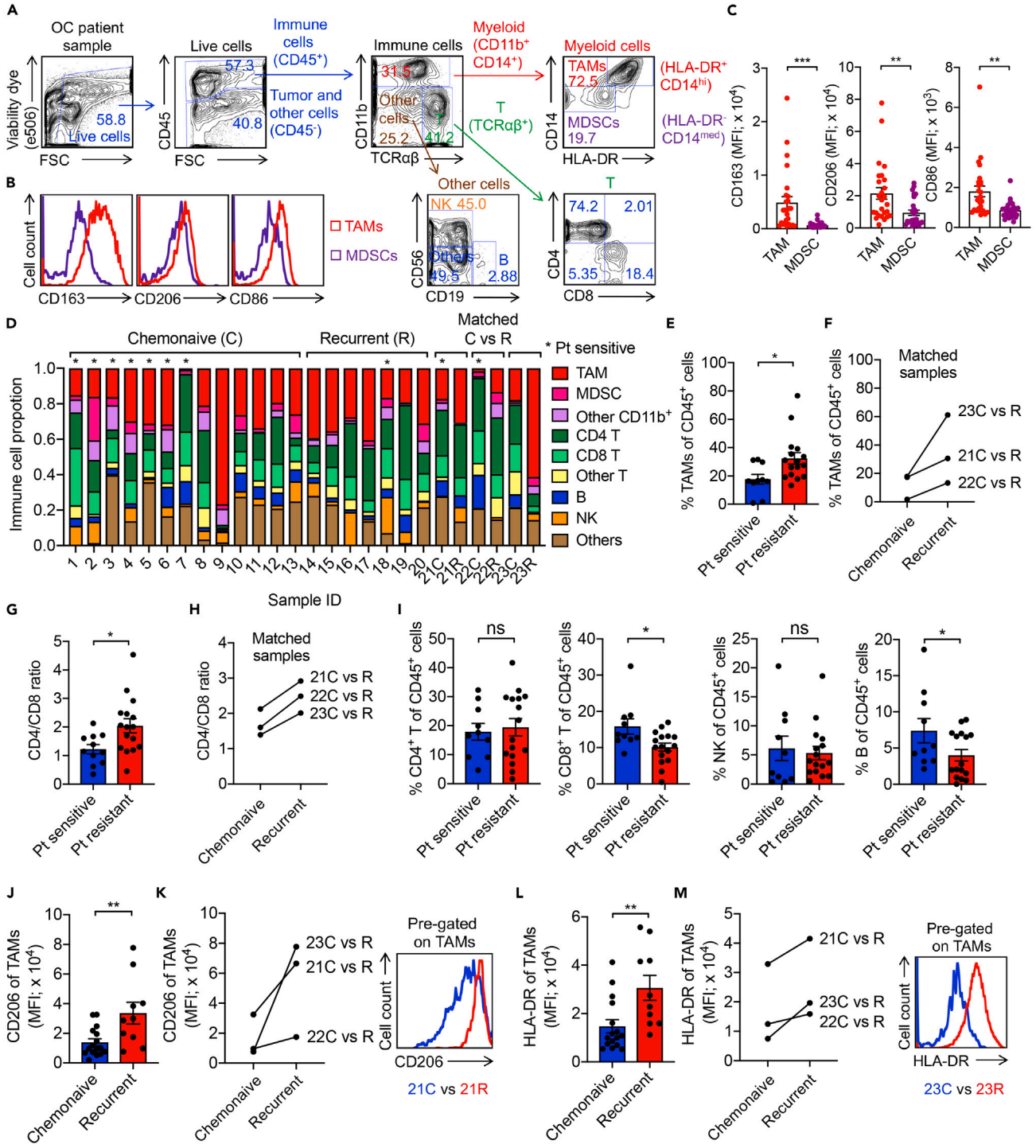

Figure 2. Profile OC tumor microenvironment (TME)

(A) Flow cytometry showing the OC patient sample-derived immune cells. Immune cells were identified as $CD45^+$ cells. TAM, tumor-associated macrophage; MDSC, myeloid-derived suppressive cell.

(B and C) FACS analyses of CD163, CD206, and CD86 expressions on TAMs and MDSCs from 26 OC samples. (B) FACS plots from one representative sample. (C) Quantification of the three marker expressions.

(D) Immune cell composition of 26 OC samples. Pt, Platinum.

(E and F) Quantification of TAM percentage of $CD45^+$ immune cells between Pt sensitive and resistant samples. Total 26 OC samples (E) and 3 paired of matched samples (F) were shown.

Figure 2. *Continued*

(G and H) Quantification of $CD4^+$ T:$CD8^+$ T ratio between Pt sensitive and resistant samples. Total 26 OC samples (G) and 3 paired of matched samples (H) were shown.

(I) Quantification of $CD4^+$ T, $CD8^+$ T, B, and NK cell percentage of $CD45^+$ immune cells between Pt sensitive and resistant samples.

(J and K) Quantification of CD206 expression on TAMs between chemonaive and recurrent samples. Total 26 OC samples (J) and 3 paired of matched samples (K) were shown.

(L and M) Quantification of HLA-DR expression on TAMs between chemonaive and recurrent samples. Total 26 OC samples (L) and 3 paired of matched samples (M) were shown. Representative of 1 (C-M) and >20 (A and B) experiments. Data are presented as the mean ± SEM. ns, not significant, *$p < 0.05$, **$p < 0.01$, ***$p < 0.001$, by Student's *t* test.

Identifying CD1d as an OC TME target for iNKT cell-based therapy

Alternative therapeutic strategies for OC patients who become platinum resistant and/or who develop tumor recurrence are needed.[1,4,7,13] One target under investigation has been the immunosuppressive network of myeloid cells in the OC TME, including TAMs and MDSCs.[22,23,65,77–80] Our ^{Allo}HSC-iNKT platform, which can target cells via NK-mediated and CD1d recognition pathways, may serve as an effective universal treatment for OC patients.[23,81–83] Thus, we evaluated the effectiveness of ^{Allo}HSC-iNKT cells against immunosuppressive myeloid cells in the TME via CD1d-mediated recognition.

Flow cytometry analysis of our OC patient samples revealed a significantly increased expression of CD1d on TAMs/MDSCs compared to other cell types, such as T cells, B cells, and NK cells (Figures 3A and 3B). Nonetheless, a degree of variability in CD1d expression was discerned across all 26 OC samples (Figure S5E). We also observed higher expression of CD1d on TAMs compared to MDSCs, indicating a plausible involvement of iNKT cells in modulating TAM activity within the OC TME (Figure 3B). Additionally, our analysis revealed that CD1d expression exhibited similarity between TAMs from chemonaive and recurrent patients (Figure 3C), implying that iNKT cells may maintain comparable efficacy in targeting the TME in both chemonaive and recurrent OC patients. Given the high expression of CD1d on TAMs/MDSCs in our OC patient samples, we have chosen to assess the efficacy of our laboratory's previously generated allogeneic hematopoietic stem cell-engineered invariant natural killer T (^{Allo}HSC-iNKT) cells[23,81–83] in targeting these particular cell populations (Figures 3D, S6A, and S6B).

Our ^{Allo}HSC-iNKT cells have already shown great promise in utilizing iNKT TCR-mediated mechanisms of action for targeting $CD1d^+$ tumor cells and inflammatory monocytes.[23,81–83] Co-culturing OC patient samples with ^{Allo}HSC-iNKT cells revealed a significant ability of ^{Allo}HSC-iNKT cells to target $CD11b^+CD1d^+$ TAMs/MDSCs from all chemonaive and recurrent OC patient samples (Figures 3E–3H, S6C, and S6D). However, ^{Allo}HSC-iNKT cells had limited effects on other immune cell subsets like T, B, and NK cells (Figure 3I), which could be due to their relatively low CD1d expression levels (Figure 3B). These results imply that the administration of ^{Allo}HSC-iNKT cell therapy holds the potential to maintain the normal immune reactivity of T, B, and NK cells.[23,81–83] Of note, the killing of TAMs/MDSCs by ^{Allo}HSC-iNKT cells was reduced when CD1d was blocked (Figures 3J and 3K), indicating that recognition of CD1d/iNKT TCR is involved in the elimination of TAMs and MDSCs. However, the use of anti-CD1d antibody did not entirely inhibit the elimination of TAMs and MDSCs (Figures 3J and 3K), suggesting the potential engagement of alternative iNKT recognition pathways, such as NKR-mediated pathways, warranting further scrutiny.[81–87]

In addition to targeting TAMs/MDSCs, our ^{Allo}HSC-iNKT cells were able to effectively target OC patient-derived tumor cells via NKRs, regardless of treatment status (Figures 3L, 3M, S6B, and S6E), highlighting the potent antitumor potential of ^{Allo}HSC-iNKT cell-based therapy for treating OC patients, particularly those who have experienced relapse following chemotherapy. In response to the robust elimination of TAMs/MDSCs and OC tumor cells, ^{Allo}HSC-iNKT cells exhibited a substantial upregulation of activation marker (i.e., CD69) and demonstrated heightened production of cytotoxic molecules (i.e., Perforin and Granzyme B) (Figure S6G). These results collectively suggest that the cytotoxic activity of ^{Allo}HSC-iNKT cells is at least partially mediated by the Perforin/Granzyme B pathway.

DISCUSSION

OC is a highly heterogeneous and devastating disease that almost certainly recurs.[1,4,5] Confounding this is the fact that many OC cases will become platinum resistant and no longer respond to traditional therapies.[7,13,88] In this case, alternative approaches that are effective in treating OC patients is an unmet clinical need.[1,4–7,12,13] Here we have profiled a series of primary OC patient samples in the hopes to better understand the antigenic and environmental factors that distinguish chemonaive from recurrent, platinum-sensitive from platinum-resistant states, and how to more effectively target OC.

During the course of OC progression, we observed an increase in the proportion of OC tumor cells expressing CSC TFs (i.e., Nanog, Oct3/4, and SOX2),[56–60] in both patient-matched and the overall cohort of recurrent OC samples (Figures 1J and 1K). The presence of CSCs in OC tumors is thought to confer resistance to certain chemotherapies and contribute to disease relapse in these patients.[19,24–31] Notably, we did not observe significant differences in the expression of surface tumor antigens that we studied, including CAR antigens (i.e., MSLN and MUC16), ESO TCR antigen (i.e., NY-ESO-1), and NK ligands (i.e., ULBPs, MICA/B, CD112, and CD155), between chemonaive and recurrent OC tumor cells (Figure 1C), suggesting that antigen-targeting cell-based therapies remain a viable option to treat these tumor cells.[14,43–48]

Another important distinction between our chemonaive and recurrent OC samples lies in the presence of a more immunosuppressive TME characterized by higher levels of TAMs and MDSCs,[18,20,21,43,89–93] along with their enhanced immunosuppressive properties (Figure 2). These TAMs and MDSCs may provide a supportive niche for CSCs and also inhibit the effectiveness of CBIs, such as T and NK cell-based

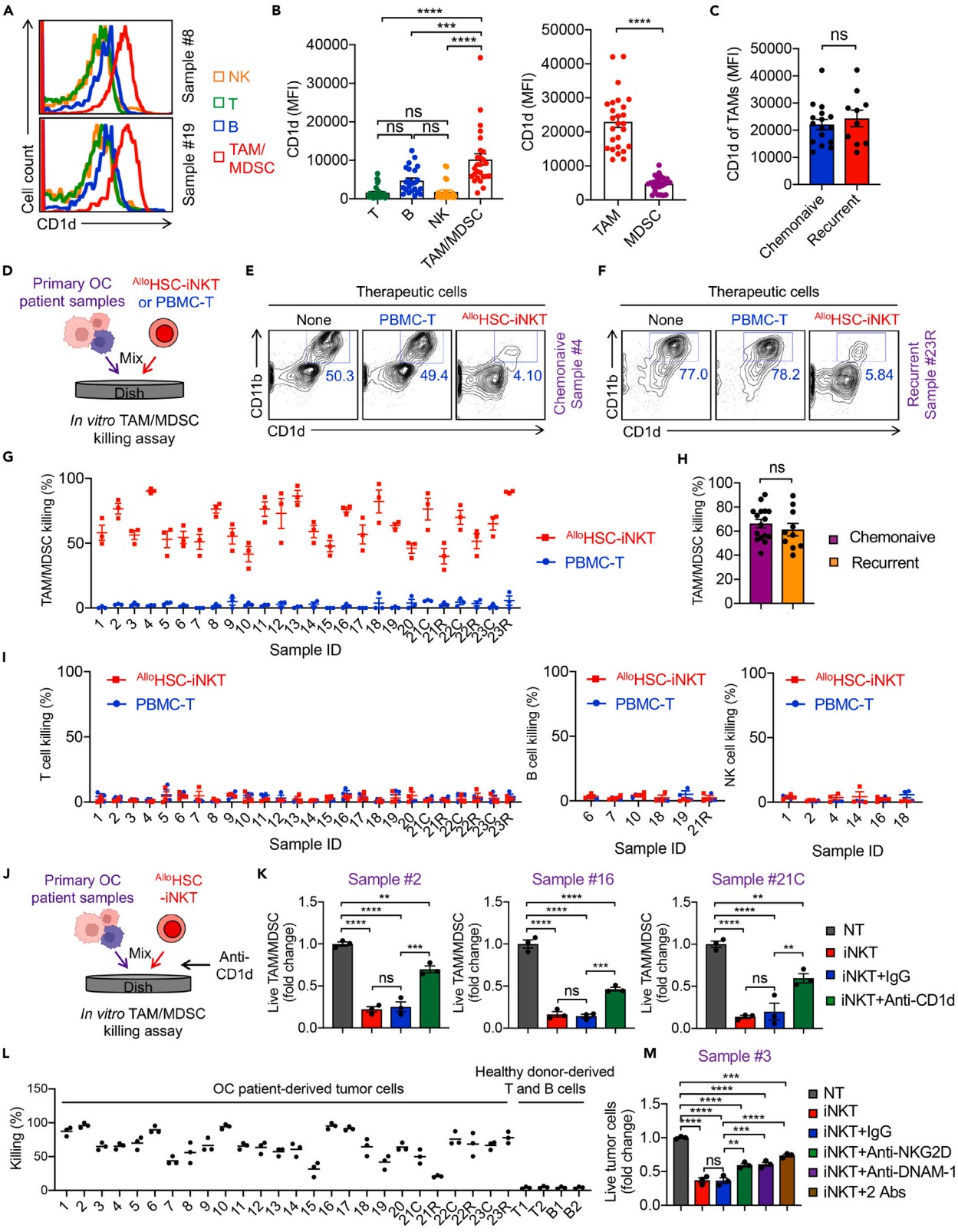
A
Sample #8
Sample #19
NK
T
B
TAM/
MDSC
Cell count
CD1d
B
CD1d (MFI)
T
B
NK
TAM/MDSC
TAM
MDSC
C
CD1d of TAMs (MFI)
Chemonaive
Recurrent
ns
D
Primary OC
patient samples
AlloHSC-iNKT
or PBMC-T
Mix
Dish
In vitro TAM/MDSC
killing assay
E
Therapeutic cells
None
PBMC-T
AlloHSC-iNKT
CD11b
CD1d
50.3
49.4
4.10
Chemonaive
Sample #4
F
Therapeutic cells
None
PBMC-T
AlloHSC-iNKT
CD11b
CD1d
77.0
78.2
5.84
Recurrent
Sample #23R
G
TAM/MDSC killing (%)
AlloHSC-iNKT
PBMC-T
Sample ID
H
TAM/MDSC killing (%)
Chemonaive
Recurrent
ns
I
T cell killing (%)
B cell killing (%)
NK cell killing (%)
AlloHSC-iNKT
PBMC-T
Sample ID
J
Primary OC
patient samples
AlloHSC
-iNKT
Mix
Anti-
CD1d
Dish
In vitro TAM/MDSC
killing assay
K
Sample #2
Sample #16
Sample #21C
Live TAM/MDSC
(fold change)
NT
iNKT
iNKT+IgG
iNKT+Anti-CD1d
L
Killing (%)
OC patient-derived tumor cells
Healthy donor-derived
T and B cells
M
Sample #3
Live tumor cells
(fold change)
NT
iNKT
iNKT+IgG
iNKT+Anti-NKG2D
iNKT+Anti-DNAM-1
iNKT+2 Abs

Figure 3. Identify CD1d as an OC TME biomarker and assess TME targeting strategy via iNKT cells

(A–C) FACS analyses of CD1d expression on the indicated immune cells. (A) CD1d expression on T, B, NK, and TAM/MDSC cells. Data from sample #8 and #19 were shown. (B) Quantification of CD1d expression on different immune cells (n = 26). (C) Quantification of CD1d expression on TAMs between chemonaive and recurrent samples. Total 26 OC samples were shown. (D-I) Studying OC TME targeting by ^{Allo}HSC-iNKT cells. Healthy donor peripheral blood mononuclear cell-derived αβ T (PBMC-T) cells were included as a therapeutic cell control.

(D) Experimental design.

(E and F) FACS analyses of live CD11b^{+}CD1d^{+} cells 24 h after co-culturing with ^{Allo}HSC-iNKT or PBMC-T cells. Data of chemonaive sample #4 (E) and recurrent sample #23R (F) were shown.

(G) TAM/MDSC killing data by ^{Allo}HSC-iNKT and PBMC-T cells at 24 h (n = 3).

(H) TAM/MDSC killing efficacy of ^{Allo}HSC-iNKT cells on chemonaive and recurrent OC samples. Data from a total 26 OC samples were shown.

(I) T, B, and NK cell killing data by ^{Allo}HSC-iNKT and PBMC-T cells at 24 h (n = 3). Results from OC samples with a high proportion of B and NK cells were presented to ensure sufficient cell numbers for analysis.

(J and K) Studying CD1d-mediated OC TME targeting by ^{Allo}HSC-iNKT cells. Anti-CD1d antibody was added into the coculture to block CD1d/iNKT TCR recognition. (J) Experimental design. (K) TAM/MDSC killing data by ^{Allo}HSC-iNKT cells at 24 h (n = 3). (L-M) Studying the tumor cell killing efficacy and mechanisms of ^{Allo}HSC-iNKT cells.

(L) Tumor cell killing data of OC tumor cells by ^{Allo}HSC-iNKT cells at 24 h (E:T = 2:1, n = 3). Healthy donor-derived T and B cells were included as target cell controls.

(M) Tumor cell killing data at 24 h (E:T = 2:1, n = 3). Anti-NKG2D and/or anti-DNAM-1 antibodies were added into the coculture to block NK receptor/ligand recognition. Representative of 1 (B, C, G-I, and L) and >20 (A, D-F, J, K, and M) experiments. Data are presented as the mean ± SEM. ns, not significant, $^{**}p < 0.01$, $^{***}p < 0.001$, by Student's *t* test (B right, C, and H), and by one-way ANOVA (B left, K, and M).

therapies.[19,22,23,26,27,32–40] Overall, our findings highlight the potential role of CSCs and immunosuppressive TME in promoting OC tumor progression and therapy resistance[19,22–31,37–40,61–63] (Figures 1J, 1K, and 2E–2M). The presence of CSCs in recurrent OC samples, coupled with the enrichment of immunosuppressive TME, underscores the need for the development of novel cell therapies that can simultaneously target tumor antigens and alter the TME.[18–21,24–31,43,89–93]

A range of strategies have been employed to target the TME in OC and other diseases, including the use of colony-stimulating factor-1 receptor (CSF-1R) inhibitors, interleukin-6 (IL-6) inhibitors, and CXCR4 antagonists to reduce the recruitment and activation of immunosuppressive cells, such as TAMs and MDSCs, in the TME.[18,39,93–95] Therefore, a multi-therapeutic strategy could prove more effective in targeting both TAMs/MDSCs and tumor cells.[65,77–79] However, these combinatorial therapeutic approaches may not be clinically feasible at the moment due to the required costs and risks of drug toxicity.[14–17,36–39,61] Given the large portion of TAMs/MDSCs in the OC TME and the increased proportion coinciding with disease recurrence, these populations of cells would make ideal targets for the goal of treating OC more effectively.[22,23,65,77–80] Notably, in this study, CD1d was identified as a targetable biomarker of the OC TME in primary patient samples and was found to be expressed at high levels on immunosuppressive TAMs and MDSCs regardless of OC disease state and platinum sensitivity (Figures 3B and 3C). Importantly, iNKT cells could specifically target CD1d-expressing TAMs and MDSCs (Figures 3E–3H) without affecting other cell types such as T, B, and NK cells (Figure 3I). Furthermore, owing to the comparatively reduced expression of CD1d on normal monocytes, the cytotoxicity of ^{Allo}HSC-iNKT cells against these healthy monocytes was markedly lower when contrasted with their cytotoxicity against TAMs and MDSCs within the TME (Figures S7A–S7E). Our study highlights the potential of CD1d as a therapeutic target for OC TME and underscores the promise of ^{Allo}HSC-iNKT cell-based therapy as a next-generation off-the-shelf medicine for this devastating disease. These findings further reinforce the need for continued research and development of innovative immunotherapeutic approaches to tackle this challenging disease.

In addition, our study provides evidence of the direct cytotoxicity of iNKT cells against OC tumor cells via NKRs, along with their ability to target the OC TME, including immunosuppressive TAMs and MDSCs, via iNKT TCR (Figures 3G, 3H, and 3L). These results underscore the therapeutic potential of iNKT cells in the treatment of OC, particularly in the challenging context of chemoresistant refractory OC tumors.[23,81–83] Notably, the expression of CAR antigens on recurrent OC tumor cells presents an opportunity for additional targeting by engineering iNKT cells to express CARs[14,43–48] (Figure 4). Moreover, our previous study demonstrated the feasibility of utilizing iNKT cells as an allogeneic off-the-shelf cell carrier for cancer treatment.[23,81–83] Collectively, our results highlight the promising role of iNKT cells as an advanced cell carrier for the next-generation off-the-shelf CBI strategies to effectively address OC, particularly in cases of recurrent OC.[23,81–83,96]

In conclusion, the development of effective therapeutic treatments for OC is imperative due to the emergence of platinum-resistant, recurrent disease.[1,4,7,13] Despite the availability of current immunotherapies for OC patients, their effectiveness is limited by the lack of uniform target surface antigen expression, the high prevalence of immunosuppressive TAMs/MDSCs, and the aggressive nature of cancer stem-like cells.[14,18–20] Our study provides a comprehensive profile of OC patient samples, encompassing both tumor cells and the TME, which serves as a roadmap for the selection of appropriate antigen targets and the development of corresponding CBIs for OC, particularly for recurrent disease (Figure 4). Furthermore, the knowledge gained from this study can be readily extended to other cancer types, particularly those exhibiting high CSC features and immunosuppressive TME.[32–35] Consequently, this research lays the foundation for the development of corresponding CBI approaches, as well as other immunotherapeutic strategies such as checkpoint blockade, monoclonal antibody therapies, and combinational therapies.

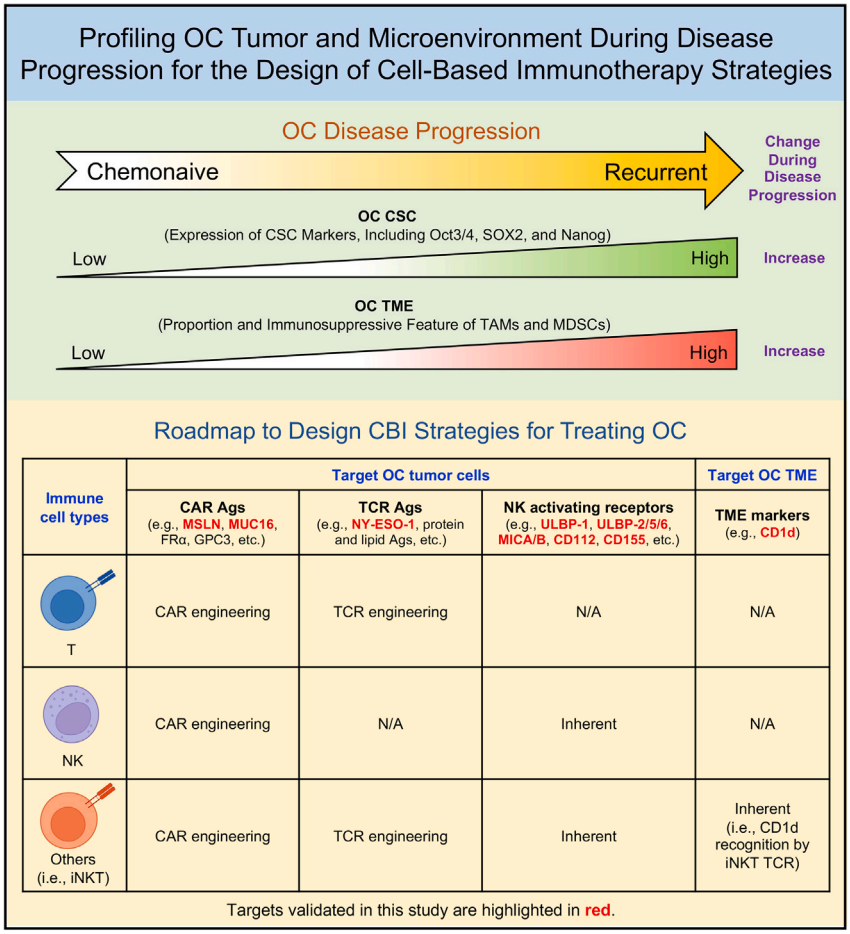

Figure 4. Summary of the OC tumor cell and TME changes during OC disease progression, and the roadmap to design the cell-based immunotherapies

Limitations of the study

Our current investigation is primarily centered around the phenotypic characterization of diverse cellular populations, such as TAMs and MDSCs, employing flow cytometry. Given the intricate array of functions and subsets inherent to these cells, including M1-like and M2-like TAMs, as well as polymorphonuclear-MDSCs versus monocytic-MDSCs, a deeper exploration into their functional attributes and more precise identification warrant further exploration. Furthermore, while our study encompasses a substantial collection of primary OC patient samples across varying platinum sensitivities and disease states, the scope of patient samples employed may present limitations. Additionally, *in vivo* modeling using patient-derived xenograft (PDX) models to validate the efficacy of CBIs may provide further evaluation, although ultimately any cell therapy efficacy can only be fully evaluated in clinical trials. There is a growing portfolio of cell-based immune therapy strategies, of which we have selectively tested some, focusing on CAR-T, TCR-T, NK, and iNKT cell-based therapies. Overall, the study provides a roadmap to design and develop new generations of CBI strategies targeting recurrent OC.

STAR★METHODS

Detailed methods are provided in the online version of this paper and include the following:

- KEY RESOURCES TABLE
- RESOURCE AVAILABILITY
  - Lead contact
  - Materials availability
  - Data and code availability
- EXPERIMENTAL MODELS AND STUDY PARTICIPANTS
  - Human Cord blood (CB) $CD34^+$ HSCs and peripheral blood mononuclear cells (PBMCs)
  - Primary ovarian cancer (OC) patient samples
  - Media and reagents

SUPPLEMENTAL INFORMATION

Supplemental information can be found online at https://doi.org/10.1016/j.isci.2023.107952.

ACKNOWLEDGMENTS

We thank the University of California, Los Angeles (UCLA) CFAR Virology Core for providing human cells and the UCLA BSCRC Flow Cytometry Core Facility for cell sorting support. This work was supported by a Partnering Opportunity for Discovery Stage Award from the California Institute for Regenerative Medicine (DISC2-13505 to L.Y.), a Broad Stem Cell Research Center Innovative Award (to L.Y. and S.M.), a Stem Cell Research Award from the Concern Foundation (to L.Y.), a Research Career Development Award from the STOP CANCER Foundation (to L.Y.), a BSCRC-RHF Research Award from the Rose Hills Research Foundation (to L.Y.), and an Ablon Scholars Award (to L.Y.). Y.-R.L. is a postdoctoral fellow supported by a UCLA MIMG M. John Pickett Post-Doctoral Fellow Award and a CIRM-BSCRC Postdoctoral Fellowship. T.S. and G.D. are supported by a VA Merit Award (5I01BX004551, to S.M.). D.L. was supported by a T32 Microbial Pathogenesis Training Grant predoctoral fellowship (Ruth L. Kirschstein National Research Service Award, T32-AI007323) and is currently supported by a T32 Tumor Immunology Training Grant postdoctoral fellowship (USHHS Ruth L. Kirschstein Institutional National Research Service Award, T32-CA009120). J.J.Z. was supported by the National Human Genome Research Institute (R01HG006139), the National Science Foundation (DMS-2054253; IIS-2205441), and the National Heart, Lung, and Blood Institute (R21HL150374).

AUTHOR CONTRIBUTIONS

Y-R.L., C.J.O, S.M., and L.Y. designed the experiments, analyzed the data, and wrote the manuscript. S.M. and L.Y. conceived and oversaw the study, with assistance from Y-R.L. and C.J.O. Y-R.L. and C.J.O performed all experiments, with assistance from Y.Z., A.K., M.W., Y.F., Y.C., T.S., G.D., E.Z., and D.L. T.S. assisted with writing the manuscript. N.A.M. verified the presence of tumor cells in histologic sections of patient samples. J.B. assisted with the screening, consenting, and collection of patient samples. J.J.Z. assisted with biostatistical analysis.

DECLARATION OF INTERESTS

Y.-R.L., D.L., and L.Y. are inventors on patents relating to this manuscript. L.Y. is a scientific advisor to AlzChem and Amberstone Biosciences and a co-founder, stockholder, and advisory board member of Appia Bio. None of the declared companies contributed to or directed any of the writing of this manuscript.

Received: June 12, 2023
Revised: August 28, 2023
Accepted: September 14, 2023
Published: September 19, 2023

REFERENCES

1. Lheureux, S., Braunstein, M., and Oza, A.M. (2019). Epithelial ovarian cancer: Evolution of management in the era of precision medicine. CA A Cancer J. Clin. *69*, 280–304. https://doi.org/10.3322/caac.21559.
2. Siegel, R.L., Miller, K.D., Wagle, N.S., and Jemal, A. (2023). Cancer statistics, 2023. CA A Cancer J. Clin. *73*, 17–48. https://doi.org/10.3322/caac.21763.
3. Sung, H., Ferlay, J., Siegel, R.L., Laversanne, M., Soerjomataram, I., Jemal, A., and Bray, F. (2021). Global Cancer Statistics 2020: GLOBOCAN Estimates of Incidence and Mortality Worldwide for 36 Cancers in 185 Countries. CA A Cancer J. Clin. *71*, 209–249. https://doi.org/10.3322/caac.21660.
4. Matulonis, U.A., Sood, A.K., Fallowfield, L., Howitt, B.E., Sehouli, J., and Karlan, B.Y. (2016). Ovarian cancer. Nat. Rev. Dis. Prim. *2*, 16061. https://doi.org/10.1038/nrdp.2016.61.

5. Reid, B.M., Permuth, J.B., and Sellers, T.A. (2017). Epidemiology of ovarian cancer: a review. Cancer Biol. Med. *14*, 9–32. https://doi.org/10.20892/j.issn.2095-3941.2016.0084.
6. Goff, B.A., Mandel, L.S., Melancon, C.H., and Muntz, H.G. (2004). Frequency of symptoms of ovarian cancer in women presenting to primary care clinics. JAMA *291*, 2705–2712. https://doi.org/10.1001/jama.291.22.2705.
7. Agarwal, R., and Kaye, S.B. (2003). Ovarian cancer: strategies for overcoming resistance to chemotherapy. Nat. Rev. Cancer *3*, 502–516. https://doi.org/10.1038/nrc1123.
8. Kurnit, K.C., Fleming, G.F., and Lengyel, E. (2021). Updates and New Options in Advanced Epithelial Ovarian Cancer Treatment. Obstet. Gynecol. *137*, 108–121. https://doi.org/10.1097/AOG.0000000000004173.
9. Marth, C., Reimer, D., and Zeimet, A.G. (2017). Front-line therapy of advanced epithelial ovarian cancer: standard treatment. Ann. Oncol. *28*, viii36–viii39. https://doi.org/10.1093/annonc/mdx450.
10. Go, R.S., and Adjei, A.A. (1999). Review of the comparative pharmacology and clinical activity of cisplatin and carboplatin. J. Clin. Oncol. *17*, 409–422. https://doi.org/10.1200/JCO.1999.17.1.409.
11. du Bois, A., Lück, H.J., Meier, W., Adams, H.P., Möbus, V., Costa, S., Bauknecht, T., Richter, B., Warm, M., Schröder, W., et al. (2003). A randomized clinical trial of cisplatin/paclitaxel versus carboplatin/paclitaxel as first-line treatment of ovarian cancer. J. Natl. Cancer Inst. *95*, 1320–1329. https://doi.org/10.1093/jnci/djg036.
12. Pignata, S., C Cecere, S., Du Bois, A., Harter, P., and Heitz, F. (2017). Treatment of recurrent ovarian cancer. Ann. Oncol. *28*, viii51–viii56. https://doi.org/10.1093/annonc/mdx441.
13. Baert, T., Ferrero, A., Sehouli, J., O'Donnell, D.M., González-Martín, A., Joly, F., van der Velden, J., Blecharz, P., Tan, D.S.P., Querleu, D., et al. (2021). The systemic treatment of recurrent ovarian cancer revisited. Ann. Oncol. *32*, 710–725. https://doi.org/10.1016/j.annonc.2021.02.015.
14. Yang, C., Xia, B.R., Zhang, Z.C., Zhang, Y.J., Lou, G., and Jin, W.L. (2020). Immunotherapy for Ovarian Cancer: Adjuvant, Combination, and Neoadjuvant. Front. Immunol. *11*, 577869. https://doi.org/10.3389/fimmu.2020.577869.
15. Nersesian, S., Glazebrook, H., Toulany, J., Grantham, S.R., and Boudreau, J.E. (2019). Naturally Killing the Silent Killer: NK Cell-Based Immunotherapy for Ovarian Cancer. Front. Immunol. *10*, 1782. https://doi.org/10.3389/fimmu.2019.01782.
16. Zhu, X., Cai, H., Zhao, L., Ning, L., and Lang, J. (2017). CAR-T cell therapy in ovarian cancer: from the bench to the bedside. Oncotarget *8*, 64607–64621. https://doi.org/10.18632/oncotarget.19929.
17. Wu, J.W.Y., Dand, S., Doig, L., Papenfuss, A.T., Scott, C.L., Ho, G., and Ooi, J.D. (2021). T-Cell Receptor Therapy in the Treatment of Ovarian Cancer: A Mini Review. Front. Immunol. *12*, 672502. https://doi.org/10.3389/fimmu.2021.672502.
18. Li, K., Shi, H., Zhang, B., Ou, X., Ma, Q., Chen, Y., Shu, P., Li, D., and Wang, Y. (2021). Myeloid-derived suppressor cells as immunosuppressive regulators and therapeutic targets in cancer. Signal Transduct. Targeted Ther. *6*, 362. https://doi.org/10.1038/s41392-021-00670-9.
19. Nowicki, A., Kulus, M., Wieczorkiewicz, M., Pieńkowski, W., Stefańska, K., Skupin-Mrugalska, P., Bryl, R., Mozdziak, P., Kempisty, B., and Piotrowska-Kempisty, H. (2021). Ovarian Cancer and Cancer Stem Cells-Cellular and Molecular Characteristics, Signaling Pathways, and Usefulness as a Diagnostic Tool in Medicine and Oncology. Cancers *13*, 4178. https://doi.org/10.3390/cancers13164178.
20. Noy, R., and Pollard, J.W. (2014). Tumor-associated macrophages: from mechanisms to therapy. Immunity *41*, 49–61. https://doi.org/10.1016/j.immuni.2014.06.010.
21. Wang, J., Cheng, F.H.C., Tedrow, J., Chang, W., Zhang, C., and Mitra, A.K. (2020). Modulation of Immune Infiltration of Ovarian Cancer Tumor Microenvironment by Specific Subpopulations of Fibroblasts. Cancers *12*, 3184. https://doi.org/10.3390/cancers12113184.
22. Wang, Y.C., Wang, X., Yu, J., Ma, F., Li, Z., Zhou, Y., Zeng, S., Ma, X., Li, Y.R., Neal, A., et al. (2021). Targeting monoamine oxidase A-regulated tumor-associated macrophage polarization for cancer immunotherapy. Nat. Commun. *12*, 3530. https://doi.org/10.1038/s41467-021-23164-2.
23. Li, Y.R., Wilson, M., and Yang, L. (2022). Target tumor microenvironment by innate T cells. Front. Immunol. *13*, 999549. https://doi.org/10.3389/fimmu.2022.999549.
24. Clevers, H. (2011). The cancer stem cell: premises, promises and challenges. Nat. Med. *17*, 313–319. https://doi.org/10.1038/nm.2304.
25. Nassar, D., and Blanpain, C. (2016). Cancer Stem Cells: Basic Concepts and Therapeutic Implications. Annu. Rev. Pathol. *11*, 47–76. https://doi.org/10.1146/annurev-pathol-012615-044438.
26. Visvader, J.E., and Lindeman, G.J. (2012). Cancer stem cells: current status and evolving complexities. Cell Stem Cell *10*, 717–728. https://doi.org/10.1016/j.stem.2012.05.007.
27. Yang, L., Shi, P., Zhao, G., Xu, J., Peng, W., Zhang, J., Zhang, G., Wang, X., Dong, Z., Chen, F., and Cui, H. (2020). Targeting cancer stem cell pathways for cancer therapy. Signal Transduct. Targeted Ther. *5*, 8. https://doi.org/10.1038/s41392-020-0110-5.
28. Nguyen, L.V., Vanner, R., Dirks, P., and Eaves, C.J. (2012). Cancer stem cells: an evolving concept. Nat. Rev. Cancer *12*, 133–143. https://doi.org/10.1038/nrc3184.
29. Silva, I.A., Bai, S., McLean, K., Yang, K., Griffith, K., Thomas, D., Ginestier, C., Johnston, C., Kueck, A., Reynolds, R.K., et al. (2011). Aldehyde dehydrogenase in combination with CD133 defines angiogenic ovarian cancer stem cells that portend poor patient survival. Cancer Res. *71*, 3991–4001. https://doi.org/10.1158/0008-5472.CAN-10-3175.
30. Wang, Y., Cardenas, H., Fang, F., Condello, S., Taverna, P., Segar, M., Liu, Y., Nephew, K.P., and Matei, D. (2014). Epigenetic targeting of ovarian cancer stem cells. Cancer Res. *74*, 4922–4936. https://doi.org/10.1158/0008-5472.CAN-14-1022.
31. Zhang, S., Balch, C., Chan, M.W., Lai, H.C., Matei, D., Schilder, J.M., Yan, P.S., Huang, T.H.M., and Nephew, K.P. (2008). Identification and characterization of ovarian cancer-initiating cells from primary human tumors. Cancer Res. *68*, 4311–4320. https://doi.org/10.1158/0008-5472.CAN-08-0364.
32. Allavena, P., Digifico, E., and Belgiovine, C. (2021). Macrophages and cancer stem cells: a malevolent alliance. Mol. Med. *27*, 121. https://doi.org/10.1186/s10020-021-00383-3.
33. Aramini, B., Masciale, V., Grisendi, G., Banchelli, F., D'Amico, R., Maiorana, A., Morandi, U., Dominici, M., and Haider, K.H. (2021). Cancer stem cells and macrophages: molecular connections and future perspectives against cancer. Oncotarget *12*, 230–250. https://doi.org/10.18632/oncotarget.27870.
34. Ge, Z., and Ding, S. (2020). The Crosstalk Between Tumor-Associated Macrophages (TAMs) and Tumor Cells and the Corresponding Targeted Therapy. Front. Oncol. *10*, 590941. https://doi.org/10.3389/fonc.2020.590941.
35. Luo, S., Yang, G., Ye, P., Cao, N., Chi, X., Yang, W.H., and Yan, X. (2022). Macrophages Are a Double-Edged Sword: Molecular Crosstalk between Tumor-Associated Macrophages and Cancer Stem Cells. Biomolecules *12*, 850. https://doi.org/10.3390/biom12060850.
36. Martinez, M., and Moon, E.K. (2019). CAR T Cells for Solid Tumors: New Strategies for Finding, Infiltrating, and Surviving in the Tumor Microenvironment. Front. Immunol. *10*, 128. https://doi.org/10.3389/fimmu.2019.00128.
37. Schweer, D., McAtee, A., Neupane, K., Richards, C., Ueland, F., and Kolesar, J. (2022). Tumor-Associated Macrophages and Ovarian Cancer: Implications for Therapy. Cancers *14*, 2220. https://doi.org/10.3390/cancers14092220.
38. DeNardo, D.G., and Ruffell, B. (2019). Macrophages as regulators of tumour immunity and immunotherapy. Nat. Rev. Immunol. *19*, 369–382. https://doi.org/10.1038/s41577-019-0127-6.
39. Xiang, X., Wang, J., Lu, D., and Xu, X. (2021). Targeting tumor-associated macrophages to synergize tumor immunotherapy. Signal Transduct. Targeted Ther. *6*, 75. https://doi.org/10.1038/s41392-021-00484-9.
40. Li, Y.R., Brown, J., Yu, Y., Lee, D., Zhou, K., Dunn, Z.S., Hon, R., Wilson, M., Kramer, A., Zhu, Y., et al. (2022). Targeting Immunosuppressive Tumor-Associated Macrophages Using Innate T Cells for Enhanced Antitumor Reactivity. Cancers *14*, 2749. https://doi.org/10.3390/cancers14112749.
41. Ahmed, N., and Stenvers, K.L. (2013). Getting to know ovarian cancer ascites: opportunities for targeted therapy-based translational research. Front. Oncol. *3*, 256. https://doi.org/10.3389/fonc.2013.00256.
42. Porcel, J.M., Diaz, J.P., and Chi, D.S. (2012). Clinical implications of pleural effusions in ovarian cancer. Respirology *17*, 1060–1067. https://doi.org/10.1111/j.1440-1843.2012.02177.x.
43. Rodriguez, G.M., Galpin, K.J.C., McCloskey, C.W., and Vanderhyden, B.C. (2018). The Tumor Microenvironment of Epithelial Ovarian Cancer and Its Influence on Response to Immunotherapy. Cancers *10*, 242. https://doi.org/10.3390/cancers10080242.
44. Paul, S., and Lal, G. (2017). The Molecular Mechanism of Natural Killer Cells Function and Its Importance in Cancer Immunotherapy. Front. Immunol. *8*, 1124. https://doi.org/10.3389/fimmu.2017.01124.
45. Baulu, E., Gardet, C., Chuvin, N., and Depil, S. (2023). TCR-engineered T cell therapy in solid tumors: State of the art and perspectives. Sci.

Adv. *9*, eadf3700. https://doi.org/10.1126/sciadv.adf3700.

46. Sterner, R.C., and Sterner, R.M. (2021). CAR-T cell therapy: current limitations and potential strategies. Blood Cancer J. *11*, 69. https://doi.org/10.1038/s41408-021-00459-7.
47. June, C.H., O'Connor, R.S., Kawalekar, O.U., Ghassemi, S., and Milone, M.C. (2018). CAR T cell immunotherapy for human cancer. Science *359*, 1361–1365. https://doi.org/10.1126/science.aar6711.
48. Shimasaki, N., Jain, A., and Campana, D. (2020). NK cells for cancer immunotherapy. Nat. Rev. Drug Discov. *19*, 200–218. https://doi.org/10.1038/s41573-019-0052-1.
49. Kalli, K.R., Oberg, A.L., Keeney, G.L., Christianson, T.J.H., Low, P.S., Knutson, K.L., and Hartmann, L.C. (2008). Folate receptor alpha as a tumor target in epithelial ovarian cancer. Gynecol. Oncol. *108*, 619–626. https://doi.org/10.1016/j.ygyno.2007.11.020.
50. Stadlmann, S., Gueth, U., Baumhoer, D., Moch, H., Terracciano, L., and Singer, G. (2007). Glypican-3 expression in primary and recurrent ovarian carcinomas. Int. J. Gynecol. Pathol. *26*, 341–344. https://doi.org/10.1097/pgp.0b013e31802d692c.
51. Tuefferd, M., Couturier, J., Penault-Llorca, F., Vincent-Salomon, A., Broët, P., Guastalla, J.P., Allouache, D., Combe, M., Weber, B., Pujade-Lauraine, E., and Camilleri-Broët, S. (2007). HER2 status in ovarian carcinomas: a multicenter GINECO study of 320 patients. PLoS One *2*, e1138. https://doi.org/10.1371/journal.pone.0001138.
52. Dillon, M.T., Bergerhoff, K.F., Pedersen, M., Whittock, H., Crespo-Rodriguez, E., Patin, E.C., Pearson, A., Smith, H.G., Paget, J.T.E., Patel, R.R., et al. (2019). ATR Inhibition Potentiates the Radiation-induced Inflammatory Tumor Microenvironment. Clin. Cancer Res. *25*, 3392–3403. https://doi.org/10.1158/1078-0432.CCR-18-1821.
53. Griesinger, L., Nyarko-Odoom, A., Martinez, S.A., Shen, N.W., Ring, K.L., Gaughan, E.M., and Mills, A.M. (2023). PD-L1 and MHC Class I Expression in High-grade Ovarian Cancers, Including Platinum-resistant Recurrences Treated With Checkpoint Inhibitor Therapy. Appl. Immunohistochem. Mol. Morphol. *31*, 197–203. https://doi.org/10.1097/PAI.0000000000001108.
54. Peng, J., Hamanishi, J., Matsumura, N., Abiko, K., Murat, K., Baba, T., Yamaguchi, K., Horikawa, N., Hosoe, Y., Murphy, S.K., et al. (2015). Chemotherapy Induces Programmed Cell Death-Ligand 1 Overexpression via the Nuclear Factor-kappaB to Foster an Immunosuppressive Tumor Microenvironment in Ovarian Cancer. Cancer Res. *75*, 5034–5045. https://doi.org/10.1158/0008-5472.CAN-14-3098.
55. Turner, T.B., Meza-Perez, S., Londoño, A., Katre, A., Peabody, J.E., Smith, H.J., Forero, A., Norian, L.A., Straughn, J.M., Jr., Buchsbaum, D.J., et al. (2017). Epigenetic modifiers upregulate MHC II and impede ovarian cancer tumor growth. Oncotarget *8*, 44159–44170. https://doi.org/10.18632/oncotarget.17395.
56. Walcher, L., Kistenmacher, A.K., Suo, H., Kitte, R., Dluczek, S., Strauß, A., Blaudszun, A.R., Yevsa, T., Fricke, S., and Kossatz-Boehlert, U. (2020). Cancer Stem Cells-Origins and Biomarkers: Perspectives for Targeted Personalized Therapies. Front. Immunol. *11*, 1280. https://doi.org/10.3389/fimmu.2020.01280.
57. Baba, T., Convery, P.A., Matsumura, N., Whitaker, R.S., Kondoh, E., Perry, T., Huang, Z., Bentley, R.C., Mori, S., Fujii, S., et al. (2009). Epigenetic regulation of CD133 and tumorigenicity of CD133+ ovarian cancer cells. Oncogene *28*, 209–218. https://doi.org/10.1038/onc.2008.374.
58. Gao, M.Q., Choi, Y.P., Kang, S., Youn, J.H., and Cho, N.H. (2010). CD24+ cells from hierarchically organized ovarian cancer are enriched in cancer stem cells. Oncogene *29*, 2672–2680. https://doi.org/10.1038/onc.2010.35.
59. Robinson, M., Gilbert, S.F., Waters, J.A., Lujano-Olazaba, O., Lara, J., Alexander, L.J., Green, S.E., Burkeen, G.A., Patrus, O., Sarwar, Z., et al. (2021). Characterization of SOX2, OCT4 and NANOG in Ovarian Cancer Tumor-Initiating Cells. Cancers *13*, 262. https://doi.org/10.3390/cancers13020262.
60. Islam, Z., Ali, A.M., Naik, A., Eldaw, M., Decock, J., and Kolatkar, P.R. (2021). Transcription Factors: The Fulcrum Between Cell Development and Carcinogenesis. Front. Oncol. *11*, 681377. https://doi.org/10.3389/fonc.2021.681377.
61. Johnson, R.L., Cummings, M., Thangavelu, A., Theophilou, G., de Jong, D., and Orsi, N.M. (2021). Barriers to Immunotherapy in Ovarian Cancer: Metabolic, Genomic, and Immune Perturbations in the Tumour Microenvironment. Cancers *13*, 6231. https://doi.org/10.3390/cancers13246231.
62. Baci, D., Bosi, A., Gallazzi, M., Rizzi, M., Noonan, D.M., Poggi, A., Bruno, A., and Mortara, L. (2020). The Ovarian Cancer Tumor Immune Microenvironment (TIME) as Target for Therapy: A Focus on Innate Immunity Cells as Therapeutic Effectors. Int. J. Mol. Sci. *21*, 3125. https://doi.org/10.3390/ijms21093125.
63. Hansen, J.M., Coleman, R.L., and Sood, A.K. (2016). Targeting the tumour microenvironment in ovarian cancer. Eur. J. Cancer *56*, 131–143. https://doi.org/10.1016/j.ejca.2015.12.016.
64. Wu, K., Lin, K., Li, X., Yuan, X., Xu, P., Ni, P., and Xu, D. (2020). Redefining Tumor-Associated Macrophage Subpopulations and Functions in the Tumor Microenvironment. Front. Immunol. *11*, 1731. https://doi.org/10.3389/fimmu.2020.01731.
65. Chen, Y., Song, Y., Du, W., Gong, L., Chang, H., and Zou, Z. (2019). Tumor-associated macrophages: an accomplice in solid tumor progression. J. Biomed. Sci. *26*, 78. https://doi.org/10.1186/s12929-019-0568-z.
66. Boutilier, A.J., and Elsawa, S.F. (2021). Macrophage Polarization States in the Tumor Microenvironment. Int. J. Mol. Sci. *22*, 6995. https://doi.org/10.3390/ijms22136995.
67. Jayasingam, S.D., Citartan, M., Thang, T.H., Mat Zin, A.A., Ang, K.C., and Ch'ng, E.S. (2019). Evaluating the Polarization of Tumor-Associated Macrophages Into M1 and M2 Phenotypes in Human Cancer Tissue: Technicalities and Challenges in Routine Clinical Practice. Front. Oncol. *9*, 1512. https://doi.org/10.3389/fonc.2019.01512.
68. Lan, C., Huang, X., Lin, S., Huang, H., Cai, Q., Wan, T., Lu, J., and Liu, J. (2013). Expression of M2-polarized macrophages is associated with poor prognosis for advanced epithelial ovarian cancer. Technol. Cancer Res. Treat. *12*, 259–267. https://doi.org/10.7785/tcrt.2012.500312.
69. Corzo, C.A., Condamine, T., Lu, L., Cotter, M.J., Youn, J.I., Cheng, P., Cho, H.I., Celis, E., Quiceno, D.G., Padhya, T., et al. (2010). HIF-1alpha regulates function and differentiation of myeloid-derived suppressor cells in the tumor microenvironment. J. Exp. Med. *207*, 2439–2453. https://doi.org/10.1084/jem.20100587.
70. Davidov, V., Jensen, G., Mai, S., Chen, S.H., and Pan, P.Y. (2020). Analyzing One Cell at a TIME: Analysis of Myeloid Cell Contributions in the Tumor Immune Microenvironment. Front. Immunol. *11*, 1842. https://doi.org/10.3389/fimmu.2020.01842.
71. Kumar, V., Patel, S., Tcyganov, E., and Gabrilovich, D.I. (2016). The Nature of Myeloid-Derived Suppressor Cells in the Tumor Microenvironment. Trends Immunol. *37*, 208–220. https://doi.org/10.1016/j.it.2016.01.004.
72. Lieber, S., Reinartz, S., Raifer, H., Finkernagel, F., Dreyer, T., Bronger, H., Jansen, J.M., Wagner, U., Worzfeld, T., Müller, R., and Huber, M. (2018). Prognosis of ovarian cancer is associated with effector memory CD8(+) T cell accumulation in ascites, CXCL9 levels and activation-triggered signal transduction in T cells. OncoImmunology *7*, e1424672. https://doi.org/10.1080/2162402X.2018.1424672.
73. Vaughan, S., Coward, J.I., Bast, R.C., Jr., Berchuck, A., Berek, J.S., Brenton, J.D., Coukos, G., Crum, C.C., Drapkin, R., Etemadmoghadam, D., et al. (2011). Rethinking ovarian cancer: recommendations for improving outcomes. Nat. Rev. Cancer *11*, 719–725. https://doi.org/10.1038/nrc3144.
74. Zhang, L., Conejo-Garcia, J.R., Katsaros, D., Gimotty, P.A., Massobrio, M., Regnani, G., Makrigiannakis, A., Gray, H., Schlienger, K., Liebman, M.N., et al. (2003). Intratumoral T cells, recurrence, and survival in epithelial ovarian cancer. N. Engl. J. Med. *348*, 203–213. https://doi.org/10.1056/NEJMoa020177.
75. Colvin, E.K. (2014). Tumor-associated macrophages contribute to tumor progression in ovarian cancer. Front. Oncol. *4*, 137. https://doi.org/10.3389/fonc.2014.00137.
76. Truxova, I., Cibula, D., Spisek, R., and Fucikova, J. (2023). Targeting tumor-associated macrophages for successful immunotherapy of ovarian carcinoma. J. Immunother. Cancer *11*, e005968. https://doi.org/10.1136/jitc-2022-005968.
77. Anfray, C., Ummarino, A., Andon, F.T., and Allavena, P. (2019). Current Strategies to Target Tumor-Associated-Macrophages to Improve Anti-Tumor Immune Responses. Cells *9*. https://doi.org/10.3390/cells9010046.
78. Li, M., He, L., Zhu, J., Zhang, P., and Liang, S. (2022). Targeting tumor-associated macrophages for cancer treatment. Cell Biosci. *12*, 85. https://doi.org/10.1186/s13578-022-00823-5.
79. Pan, Y., Yu, Y., Wang, X., and Zhang, T. (2020). Tumor-Associated Macrophages in Tumor Immunity. Front. Immunol. *11*, 583084. https://doi.org/10.3389/fimmu.2020.583084.
80. Rao, R., Han, R., Ogurek, S., Xue, C., Wu, L.M., Zhang, L., Zhang, L., Hu, J., Phoenix, T.N., Waggoner, S.N., and Lu, Q.R. (2022). Glioblastoma genetic drivers dictate the function of tumor-associated macrophages/microglia and responses to CSF1R inhibition. Neuro Oncol. *24*, 584–597. https://doi.org/10.1093/neuonc/noab228.
81. Li, Y.R., Dunn, Z.S., Garcia, G., Jr., Carmona, C., Zhou, Y., Lee, D., Yu, J., Huang, J., Kim, J.T., Arumugaswami, V., et al. (2022). Development of off-the-shelf hematopoietic stem cell-engineered invariant natural killer

T cells for COVID-19 therapeutic intervention. Stem Cell Res. Ther. *13*, 112. https://doi.org/10.1186/s13287-022-02787-2.

82. Li, Y.R., Zeng, S., Dunn, Z.S., Zhou, Y., Li, Z., Yu, J., Wang, Y.C., Ku, J., Cook, N., Kramer, A., and Yang, L. (2022). Off-the-shelf third-party HSC-engineered iNKT cells for ameliorating GvHD while preserving GvL effect in the treatment of blood cancers. iScience *25*, 104859. https://doi.org/10.1016/j.isci.2022.104859.
83. Li, Y.R., Zhou, Y., Kim, Y.J., Zhu, Y., Ma, F., Yu, J., Wang, Y.C., Chen, X., Li, Z., Zeng, S., et al. (2021). Development of allogeneic HSC-engineered iNKT cells for off-the-shelf cancer immunotherapy. Cell Rep. Med. *2*, 100449. https://doi.org/10.1016/j.xcrm.2021.100449.
84. Bendelac, A., Savage, P.B., and Teyton, L. (2007). The biology of NKT cells. Annu. Rev. Immunol. *25*, 297–336. https://doi.org/10.1146/annurev.immunol.25.022106.141711.
85. Brennan, P.J., Brigl, M., and Brenner, M.B. (2013). Invariant natural killer T cells: an innate activation scheme linked to diverse effector functions. Nat. Rev. Immunol. *13*, 101–117. https://doi.org/10.1038/nri3369.
86. Kronenberg, M. (2005). Toward an understanding of NKT cell biology: progress and paradoxes. Annu. Rev. Immunol. *23*, 877–900. https://doi.org/10.1146/annurev.immunol.23.021704.115742.
87. Van Kaer, L., Parekh, V.V., and Wu, L. (2011). Invariant natural killer T cells: bridging innate and adaptive immunity. Cell Tissue Res. *343*, 43–55. https://doi.org/10.1007/s00441-010-1023-3.
88. Singh, T., Neal, A., Dibernardo, G., Raheseparian, N., Moatamed, N.A., and Memarzadeh, S. (2022). Efficacy of birinapant in combination with carboplatin in targeting platinum-resistant epithelial ovarian cancers. Int. J. Oncol. *60*, 35. https://doi.org/10.3892/ijo.2022.5325.
89. Aziz, M.A.A.E., Agarwal, K., Dasari, S., and Mitra, A.A.K. (2019). Productive Cross-Talk with the Microenvironment: A Critical Step in Ovarian Cancer Metastasis. Cancers *11*, 1608. https://doi.org/10.3390/cancers11101608.
90. Cummings, M., Freer, C., and Orsi, N.M. (2021). Targeting the tumour microenvironment in platinum-resistant ovarian cancer. Semin. Cancer Biol. *77*, 3–28. https://doi.org/10.1016/j.semcancer.2021.02.007.
91. Dasari, S., Fang, Y., and Mitra, A.K. (2018). Cancer Associated Fibroblasts: Naughty Neighbors That Drive Ovarian Cancer Progression. Cancers *10*, 406. https://doi.org/10.3390/cancers10110406.
92. Lan, C., Heindl, A., Huang, X., Xi, S., Banerjee, S., Liu, J., and Yuan, Y. (2015). Quantitative histology analysis of the ovarian tumour microenvironment. Sci. Rep. *5*, 16317. https://doi.org/10.1038/srep16317.
93. Yang, Y., Yang, Y., Yang, J., Zhao, X., and Wei, X. (2020). Tumor Microenvironment in Ovarian Cancer: Function and Therapeutic Strategy. Front. Cell Dev. Biol. *8*, 758. https://doi.org/10.3389/fcell.2020.00758.
94. Mabuchi, S., Sasano, T., and Komura, N. (2021). Targeting Myeloid-Derived Suppressor Cells in Ovarian Cancer. Cells. https://doi.org/10.3390/cells10020329.
95. Pathria, P., Louis, T.L., and Varner, J.A. (2019). Targeting Tumor-Associated Macrophages in Cancer. Trends Immunol. *40*, 310–327. https://doi.org/10.1016/j.it.2019.02.003.
96. Li, Y.R., Dunn, Z.S., Yu, Y., Li, M., Wang, P., and Yang, L. (2023). Advancing cell-based cancer immunotherapy through stem cell engineering. Cell Stem Cell *30*, 592–610. https://doi.org/10.1016/j.stem.2023.02.009.
97. Giannoni, F., Hardee, C.L., Wherley, J., Gschweng, E., Senadheera, S., Kaufman, M.L., Chan, R., Bahner, I., Gersuk, V., Wang, X., et al. (2013). Allelic exclusion and peripheral reconstitution by TCR transgenic T cells arising from transduced human hematopoietic stem/progenitor cells. Mol. Ther. *21*, 1044–1054. https://doi.org/10.1038/mt.2013.8.
98. Lan, P., Tonomura, N., Shimizu, A., Wang, S., and Yang, Y.G. (2006). Reconstitution of a functional human immune system in immunodeficient mice through combined human fetal thymus/liver and CD34+ cell transplantation. Blood *108*, 487–492. https://doi.org/10.1182/blood-2005-11-4388.
99. Zhu, Y., Smith, D.J., Zhou, Y., Li, Y.R., Yu, J., Lee, D., Wang, Y.C., Di Biase, S., Wang, X., Hardoy, C., et al. (2019). Development of Hematopoietic Stem Cell-Engineered Invariant Natural Killer T Cell Therapy for Cancer. Cell Stem Cell *25*, 542–557.e9. https://doi.org/10.1016/j.stem.2019.08.004.

STAR★METHODS

KEY RESOURCES TABLE

REAGENT or RESOURCE	SOURCE	IDENTIFIER
Antibodies		
Anti-human CD45 (Clone H130)	Biolegend	CAT#304026, RFID: AB_893337
Anti-human TCR αβ (Clone I26)	Biolegend	CAT#306716, RRID: AB_1953257
Anti-human TCR Vβ13.1 (Clone H131)	Biolegend	CAT#362403, RRID: AB_2564031
Anti-human CD4 (Clone OKT4)	Biolegend	CAT#317414, RRID: AB_571959
Anti-human CD8 (Clone SK1)	Biolegend	CAT#344714, RRID: AB_2044006
Anti-human CD19 (Clone SJ25C1)	Biolegend	CAT#363005, RRID: AB_2564127
Anti-human CD31 (Clone WM59)	Biolegend	CAT#303117, RRID: AB_2114314
Anti-human CD34 (Clone 581)	Biolegend	CAT#555822, RRID: AB_396151
Anti-human CD44 (Clone BJ18)	Biolegend	CAT#397503, RRID: AB_2814372
Anti-human CD24 (Clone ML5)	Biolegend	CAT#311113, RRID: AB_2561283
Anti-human CD133 (Clone clone7)	Biolegend	CAT#372805, RRID: AB_2632881
Anti-human CD117 (Clone 104D2)	Biolegend	CAT#313227, RRID: AB_2566214
Anti-human CD112 (Clone TX31)	Biolegend	CAT#337409, RRID: AB_2174163
Anti-human CD155 (Clone SKII.4)	Biolegend	CAT#337613, RRID: AB_2565746
Anti-human CD14 (Clone HCD14)	Biolegend	CAT#325608, RRID: AB_830681
Anti-human CD1d (Clone 51.1)	Biolegend	CAT#350308, RRID: AB_10642829
Anti-human CD11b (Clone ICRF44)	Biolegend	CAT#301330, RRID: AB_2561703
Anti-human CD56 (Clone HCD56)	Biolegend	CAT#362545, RRID: AB_2565963
Anti-human CD206 (Clone 15-2)	Biolegend	CAT#321110, RRID: AB_571885
Anti-human CD163 (Clone GHI/61)	Biolegend	CAT#333621, RRID: AB_2563611
Anti-human CD86 (Clone IT2.2)	Biolegend	CAT#374209, RRID: AB_2728391
Anti-human NKp30 (Clone P30-15)	Biolegend	CAT#325207, RRID: AB_756111
Anti-human NKp44 (Clone P44-8)	Biolegend	CAT#325107, RRID: AB_756099
Anti-human NKG2D (Clone 1D11)	Biolegend	CAT#320812, RRID: AB_2234394
Anti-human DNAM-1 (Clone 11A8)	Biolegend	CAT#338312, RRID: AB_2561952
Anti-human Granzyme B (Clone QA16A02)	Biolegend	CAT#372204, RRID: AB_2687028
Anti-human Perforin (Clone dG9)	Biolegend	CAT#308126, RRID: AB_2572049
Anti-human b2-microglobulin (B2M) (Clone 2M2)	Biolegend	CAT#316312, RRID: AB_10641281
Anti-human HLA-DR (Clone L243)	Biolegend	CAT#307618, RRID: AB_493586
Anti-human HLA-A,B,C (Clone W6/32)	Biolegend	CAT#311421, RRID: AB_1501265
Anti-human MICA/MICB (Clone 6D4)	Biolegend	CAT#320908, RRID: AB_493195
Anti-human CTAG1B (W19067B)	Biolegend	CAT#382302, RRID: AB_2922615
Anti-human CA125 (Clone 618F)	Biolegend	CAT#666904, RRID: AB_2629540
Anti-SOX2 (Clone 14A6A34)	Biolegend	CAT#656112, RRID: AB_2566189
Anti-Oct3/4 (Clone 3A2A20)	Biolegend	CAT#653704, RRID: AB_2562018
LEAF purified anti-human NKG2D antibody (Clone 1D11)	Biolegend	CAT#320810, RRID: AB_2133276
LEAF purified anti-human CD1d antibody (Clone 51.1)	Biolegend	CAT#350304, RRID: AB_10641291
Mouse IgG1, k isotype control antibody (Clone MOPC-21)	Biolegend	CAT#400124, RRID: AB_2890215
LEAF purified Mouse IgG2b, k isotype ctrl (Clone MG2b-57)	Biolegend	CAT#401201, RRID: AB_2744505
Human Fc Receptor Blocking Solution (TrueStain FcX)	Biolegend	CAT#422302, RRID: AB_2818986

(*Continued on next page*)

Continued

REAGENT or RESOURCE	SOURCE	IDENTIFIER
Goat anti-mouse IgG (minimal x-reactivity) Antibody	Biolegend	CAT#405305, RRID: AB_315008
Goat anti-rat IgG (minimal x-reactivity) Antibody	Biolegend	CAT#405413, RRID: AB_10661733
Donkey anti-rabbit IgG (minimal x-reactivity) Antibody	Biolegend	CAT#406421, RRID: AB_2563484
Streptavidin	Biolegend	CAT#405207
Anti-human TCR Va24-Jb18 (Clone 6B11)	BD Biosciences	CAT#552825, RRID: AB_394478
LEAF purified anti-human DNAM-1 antibody (Clone DX11)	BD Biosciences	CAT#559786, RRID: AB_397327
Mouse Fc Block (anti-mouse CD16/32)	BD Biosciences	CAT#553142, RRID: AB_394657
Anti-human mesothelin (MSLN) (Clone 420411)	R&D Systems	CAT#FAB32652P, RRID: AB_1151946
Anti-human fibroblast activation protein alpha/FAP (Clone 427819)	R&D Systems	CAT# MAB3715-SP
Anti-human ULBP-1 (Clone 170818)	R&D Systems	CAT#FAB1380P, RRID: AB_2687471
Anti-human ULBP-2,5,6 (Clone 165903)	R&D Systems	CAT#FAB1298A, RRID: AB_2257142
Goat anti-Mouse IgG F(ab')2 Secondary Antibody, Biotin	ThermoFisher	CAT#31803, RRID: AB_228311
Anti-Nanog (Clone EPR2027-2)	Abcam	CAT#ab109250, RRID: AB_10863442
Anti-human Vβ11	Beckman-Coulter	CAT#A66905
Bacterial and virus strains		
Lenti/iNKT-sr39TK	This paper	N/A
Lenti/MCAR	This paper	N/A
Lenti/1G4-TK	This paper	N/A
Biological samples		
Human peripheral blood mononuclear cells (PBMCs)	UCLA	N/A
Human cord blood $CD34^+$ hematopoietic stem and progenitor cells (HSCs)	UCLA	N/A
Human ovarian cancer patient samples	UCLA	N/A
Chemicals, peptides, and recombinant proteins		
Streptavidin-HRP conjugate	Invitrogen	CAT#SA10001
Recombinant human IL-2	Peprotech	CAT#200–02
Recombinant human IL-3	Peprotech	CAT#200–03
Recombinant human IL-7	Peprotech	CAT#200–07
Recombinant human IL-15	Peprotech	CAT#200–15
Recombinant human Flt3-Ligand	Peprotech	CAT#300–19
Recombinant human SCF	Peprotech	CAT#300–07
Recombinant human TPO	Peprotech	CAT#300–18
Recombinant human GM-CSF	Peprotech	CAT#300–03
L-ascorbic acid 2-phosphate	Sigma	CAT#A8960-5G
B27" Supplement (50X), serumfree	ThermoFisher	CAT#17504044
a-Galactosylceramide (KRN7000)	Avanti Polar Lipids	SKU#867000P-1mg
X-VIVO 15 Serum-free Hematopoietic Cell Medium	Lonza	CAT#04–418Q
UltraCULTURE media	Lonza	CAT#BP12725F
RPMI1640 cell culture medium	Corning Cellgro	CAT#10-040-CV
DMEM cell culture medium	Corning Cellgro	CAT#10-013-CV
Fetal Bovine Serum (FBS)	Sigma	CAT#F2442
MACS BSA stock solution	Miltenyi	CAT#130-091-376
30% BSA	Gemini	CAT#50-753-3079
Penicillin-Streptomycine-Glutamine (P/S/G)	Gibco	CAT#10378016
Penicillin: streptomycin (pen:strep) solution (P/S)	Gemini Bio-products	CAT#400–109

(*Continued on next page*)

Continued

REAGENT or RESOURCE	SOURCE	IDENTIFIER
MEM non-essential amino acids (NEAA)	Gibco	CAT#11140050
HEPES Buffer Solution	Gibco	CAT#15630056
Sodium Pyruvate	Gibco	CAT#11360070
Beta-Mercaptoethanol	Sigma	SKU#M6250
Normocin	InvivoGen	CAT#ant-nr-2
Cell Fixation/Permeabilization Kit	BD Biosciences	CAT#554714
RetroNectin recombination human fibronectin fragment, 2.5mg	Takara	CAT#T100B
Phosphate Buffered Saline (PBS) pH 7.4 (1X)	Gibco	CAT#10010–023
Poloxamer Synperonic F108	Sigma	CAT#07579–250G-F
Prostaglandin E2	Cayman Chemical	CAT#14-190-1
Collagenase-Type I	ThermoFisher	CAT#17100017
Dispase II	ThermoFisher	CAT#17105041
DNase I	Sigma-Aldrich	CAT #10104159001
Fixable Viability Dye eFluor506 affymetrix	eBioscience	CAT#65-0866-14
Critical commercial assays		
Human CD34 MicroBeads Kit	Miltenyi Biotec	CAT#130-046-703
Human CD14 MicroBeads Kit	Miltenyi Biotec	CAT#130-050-201
Human Anti-iNKT MicroBeads	Miltenyi Biotec	CAT#130-094-842
Human tumor cell isolation kit	Miltenyi Biotec	CAT#130-108-339
Fixation/Permeabilization Solution Kit	BD Sciences	CAT#55474
Foxp3 / Transcription Factor Staining Buffer Set	eBioscience	CAT#00-5523-00
StemSpan™™ Lymphoid Differentiation Coating Material (100X)	Stem Cell Technologies	CAT#9925
StemSpan™ SFEM II	Stem Cell Technologies	CAT#9605
ImmunoCult" Human CD3/CD28/CD2 T Cell Activator	Stem Cell Technologies	CAT#10970
TransIT-Lenti Transfection Reagent	Mirus Bio	CAT#MIR 6600
Amicon Ultra-15 Centrifugal Filter Unit	Millipore Sigma	CAT#UFC910024
Cryostor cell cryopreservation media	Sigma	CAT#C2874-100ML
Recombinant DNA		
Vector: parental lentivector pMNDW	[97,98]	N/A
Software and algorithms		
FlowJo Software 9	FlowJo	https://www.flowjo.com/solutions/flowjo/downloads
Prism 8	Graphpad	https://www.graphpad.com/scientific-software/prism/

RESOURCE AVAILABILITY

Lead contact

Further information and requests for new reagents generated in this study may be directed to, and will be fulfilled by the lead contact, Lili Yang (liliyang@ucla.edu).

Materials availability

All unique/stable reagents generated in this study are available from the lead contact with a completed Materials Transfer Agreement.

Data and code availability

- All data reported in this manuscript are available from the lead contact without restriction.
- No custom computer code was reported in this manuscript.

- Any additional information required to reanalyze the data reported in this paper is available from the lead contact on request.

EXPERIMENTAL MODELS AND STUDY PARTICIPANTS

Human Cord blood (CB) CD34$^+$ HSCs and peripheral blood mononuclear cells (PBMCs)

Purified CB CD34$^+$ cells were purchased from HemaCare, and isolated through magnetic-activated cell sorting using ClinMACs CD34$^+$ microbeads (Miltenyi Biotech; Auburn, CA, USA). Healthy donor human PBMCs were obtained from the UCLA/CFAR Virology Core Laboratory, without identification information under federal and state regulations. Cells were cryopreserved in Cryostor CS10 (Sigma St. Louis, MO, USA) using CoolCell (BioCision, Larkspur, CA, UCA), and were frozen in liquid nitrogen for all experiments and long-term storage.

Primary ovarian cancer (OC) patient samples

This study was approved by the UCLA Office of the Human Research Protection Program, IRB #10-000727 and IRB #20-001659. Primary OC patient samples were collected from consented patients through an IRB-approved protocol (IRB #10-000727) and processed.

Media and reagents

α-Galactosylceramide (αGC, KRN7000) was purchased from Avanti Polar Lipids (Alabaster, AL, USA). Recombinant human IL-2, IL-3, IL-7, IL-15, Flt3-ligand (FLT3-L), stem cell factor (SCF), and thrombopoietin (TPO) were purchased from PeproTech (Hamburg, Germany).

X-VIVO 15 Serum-free Hematopoietic Cell Medium was purchased from Lonza (Bend, OR, USA). RPMI1640 and DMEM cell culture medium were purchased from Corning Cellgro (Manassas, VA, USA). Fetal bovine serum (FBS) and Beta-Mercaptoethanol (β-ME) were purchased from Sigma. Medium supplements, including Penicillin-Streptomycin-Glutamine (P/S/G), MEM non-essential amino acids (NEAA), HEPES Buffer Solution, and Sodium Pyruvate, were purchased from GIBCO (Waltham, MA, USA). Normocin was purchased from InvivoGen (San Diego, CA, USA). Complete lymphocyte culture medium (denoted as C10 medium) was made of RPMI 1640 supplemented with FBS (10% vol/vol), P/S/G (1% vol/vol), MEM NEAA (1% vol/vol), HEPES (10 mM), Sodium Pyruvate (1 mM), β-ME (50 μM), and Normocin (100 μg/mL). Adherent cell culture medium (denoted as D10 medium) was made of DMEM supplemented with FBS (10% vol/vol), P/S/G (1% vol/vol), and Normocin (100 μg/mL).

METHOD DETAILS

Lentiviral vectors and transduction

Lentiviral vectors used in this study were all constructed from a parental lentivector pMNDW.[83,99] The Lenti/MCAR vector was constructed by inserting a synthetic gene encoding mesothelin-targeting chimeric antigen receptor (MCAR) into pMNDW. The MCAR design contains a mesothelin-targeting single-chain variable fragment (scFv), a CD8 hinge, a CD28 transmembrane domain, a CD28 and 4-1BB co-stimulatory domain, and a CD3ζ domain. The Lenti/1G4-TK vector was constructed by inserting a tricistronic synthetic gene encoding human NY-ESO-1-specific HLA-A2.01-restricted TCRα-F2A-TCRβ-P2A-sr39TK into pMNDW; the Lenti/iNKT-sr39TK vector was constructed by inserting a synthetic tricistronic gene encoding human iNKT TCRα-F2A-TCRβ-P2A-sr39TK into pMNDW. The synthetic gene fragments were obtained from GenScript (Piscataway, NJ, USA) or IDT (Coralville, IA, USA). Lentiviruses were produced using HEK-293T cells following a standard transfection protocol. Briefly, HEK-293T cells were co-transfected with three plasmids: a lentiviral vector plasmid, a lentiviral glycoprotein plasmid (pCMV-VSVG), and a lentiviral packaging plasmid (pCMV-Delta R8.9), using TransIT-Lenti Transfection Reagent (Mirus Bio; Cat. MIR 6600) for 16 to 18 hours. This was followed by treatment with 10 mM sodium butyrate for 8 hours. Subsequently, virus-containing supernatants were generated in serum-free UltraCULTURE media (Lonza Walkersville; Cat. BP12725F) for 48 hours. The supernatants were concentrated using a 100KDa Amicon Ultra-15 Centrifugal Filter Unit (Millipore Sigma; Cat. UFC910024) at 4000 rcf for 40 minutes at 4°C, and stored as aliquots at -80°C. Lentivector titers were measured by transducing HEK-293T cells with serial dilutions and performing flow cytometry.

Primary patient sample collection and processing

OC patient samples were initially collected, spun down, and red blood cell (RBC) lysis was performed using BioLegend's RBC lysis protocol (BioLegend, San Diego, CA, USA, CAT #420302). Following RBC lysis, cells either proceeded to be analyzed fresh or were resuspended after RBC lysis in a cryopreservation buffer and stored in liquid nitrogen for later experimental use. All samples, both fresh and cryopreserved, were enzymatically digested using 2 mg/mL collagenase-Type I (ThermoFisher Scientific, Waltham, MA, USA, CAT #17100017) and 2 mg/mL dispase II (ThermoFisher Scientific, CAT #17105041) solution, supplemented with 1mg/mL DNase I (Sigma-Aldrich, CAT #10104159001) for 60 min at 37°C while rotating. For samples analyzed after cryopreservation, resuscitation consisted of first washing cells with DMEM supplemented with FBS (10% vol/vol) and P/S/G (1% vol/vol). In total, 16 chemonaive and 10 recurrent patient samples were used in the analysis. Samples were either derived from ascites or pleural fluid sources.

Classification of platinum sensitivity in OC patient samples and treatment status

A prospective assessment of chemonaive OC patients was taken to determine platinum sensitivity status based on disease recurrence. In following the treatment status of chemonaive OC patients, if disease relapse was seen < 6 months following the last infusion of platinum-based chemotherapy, the sample collected was classified as platinum resistant. Samples collected from patients for whom disease relapse

was seen ≥ 6 months after the last infusion of platinum-based chemotherapy were considered platinum sensitive. A retrospective assessment of a patient's previous treatment history was used to classify platinum sensitivity of recurrent patient samples. Those samples that were collected from patients who experienced a recurrence of disease within < 6 months of the last infusion of platinum-based chemotherapy were annotated as platinum resistant. In addition, patients who had evidence of disease progression on platinum therapy were classified as platinum resistant. While samples collected from patients who experienced disease recurrence at a time ≥ 6 months following the last infusion of platinum-based chemotherapy were classified as platinum sensitive.

Antibodies and flow cytometry

The samples were stained with Fixable Viability Dye eFluor506 (e506) mixed with Mouse Fc Block (anti-mouse CD16/32) or Human Fc Receptor Blocking Solution (TrueStain FcX) prior to antibody staining. Antibody staining was performed at a dilution according to the manufacturer's instructions. Fluorochrome-conjugated antibodies specific for human CD45 (Clone H130, PerCP or Pacific Blue-conjugated, 1:500), TCR αβ (Clone I26, Pacific Blue or PE-Cy7-conjugated, 1:25), TCR Vβ13.1 (Clone H131, FITC-conjugated, 1:100), CD4 (Clone OKT4, PE-Cy7, Pacific Blue, or FITC-conjugated, 1:400), CD8 (Clone SK1, APC-Cy7, PerCP, or PE-conjugated, 1:500), CD31 (Clone WM59, PE-Cy7-conjugated, 1:100), CD34 (Clone 581, PE-conjugated, 1:500), CD44 (Clone BJ18, PE-conjugated, 1:2000), CD24 (Clone ML5, PerCP-conjugated, 1:500), CD133 (Clone clone7, APC-conjugated, 1:500), CD117 (Clone 104D2, APC-Cy7-conjugated, 1:25), CD112 (Clone TX31, PE-conjugated, 1:50), CD155 (Clone SKII.4, PE-Cy7-conjugated, 1:250), CD56 (Clone HCD56, PerCP or FITC-conjugated, 1:10), CD14 (Clone HCD14, Pacific Blue-conjugated, 1:100), CD1d (Clone 51.1, APC or PE-Cy7-conjugated, 1:50), CD11b (clone ICRF44, PE or FITC-conjugated, 1:3000), CD206 (Clone 15-2, APC-conjugated, 1:500), CD163 (Clone GHI/61, APC-Cy7-conjugated, 1:500), CD86 (Clone IT2.2, PE-Cy7-conjugated, 1:100), CD19 (Clone HIB19, APC-Cy7-conjugated, 1:150), NKG2D (Clone 1D11, PE-Cy7-conjugated, 1:50), DNAM-1 (Clone 11A8, APC-conjugated, 1:50), NKp30 (Clone P30-15, PE-conjugated, 1:50), NKp44 (Clone P44-8, PE-conjugated, 1:50), β2-microglobulin (B2M) (Clone 2M2, FITC or APC-conjugated, 1:8000), HLA-A,B,C (Clone W6/32, PerCP-conjugated, 1:500), HLA-DR (Clone L243, APC-Cy7-conjugated, 1:500), MICA/MICB (Clone 6D4, APC-conjugated, 1:25), CTAG1B (W19067B, fluorochrome-unconjugated, 1:100), CA125 (Clone 618F, fluorochrome-unconjugated, 1:100), SOX2 (Clone 14A6A34, Pacific Blue-conjugated, 1:100), Oct3/4 (Clone 3A2A20, PE-conjugated, 1:100) and Streptavidin (APC-conjugated, 1:1000) were purchased from BioLegend; Fluorochrome-conjugated antibodies specific for human mesothelin (MSLN) (Clone 420411, PE-conjugated, 1:10), fibroblast activation protein alpha/FAP (Clone 427819, fluorochrome-unconjugated, 1:100), ULBP-1 (Clone 170818, PE-conjugated, 1:25) and ULBP-2,5,6 (Clone 165903, APC-conjugated, 1:25) were purchased from R&D Systems (Minneapolis, MN, USA); Fluorochrome-conjugated antibodies specific for mouse IgG (Clone Poly4053, Pacific Blue or FITC-conjugated, 1:500), rat IgG (Clone Poly4054, PE-Cy7-conjugated, 1:500), and rabbit IgG (Clone Poly4064, PE or FITC-conjugated, 1:500) were purchased from Biolegend; PE-conjugated antibodies specific for TCR Vα24-Jβ18 (Clone 6B11, 1:10) were purchased from BD Biosciences (San Jose, CA, USA). Fixable Viability Dye e506 (1:500) was purchased from Affymetrix eBioscience. Human Fc Receptor Blocking Solution (TruStain FcX, 1:100) was purchased from BioLegend, and Mouse Fc Block (anti-mouse CD16/32, 1:50) was purchased from BD Biosciences. Intracellular cytokines were stained using a Cell Fixation/Permeabilization Kit (BD Biosciences, CAT #554714). Transcription factors were stained using a Foxp3/Transcription Factor Staining Buffer Set (Thermofisher Scientific, CAT #00-5523-00), following manufacturer's instructions. Goat anti-mouse IgG F(ab')2 secondary antibody (1:50) was purchased from ThermoFisher Scientific. A recombinant antibody specific for human Nanog (Clone EPR2027-2, fluorochrome-unconjugated, 1:3000) was purchased from Abcam (Cambridge, UK). An APC-conjugated antibody specific for human Vβ11 (1:200) was purchased from Beckman-Coulter (Brea, CA, USA). Flow cytometry analysis was conducted using a MACSQuant Analyzer 10 flow cytometer (Miltenyi Biotech). Data acquisition and analysis were performed using FlowJo software version 9. Gating strategies and fluorescence compensation settings were established based on appropriate controls, including isotype controls. The percentage of specific cell populations was determined by gating on antibody-stained samples and isotype control stained samples. The Mean or Median Fluorescence Intensity of specific markers within cell populations was calculated using FlowJo software version 9. Statistical analyses were performed using Student's *t*-test or one-way ANOVA.

In vitro generation of allogeneic HSC-Engineered iNKT (^{Allo}HSC-iNKT) cells

Cord blood-derived human CD34$^+$ HSCs were obtained from HemaCare and thawed and recovered in X-VIVO 15 Serum-Free Hematopoietic Stem Cell medium supplemented with human recombinant SCF (50 ng/mL), FLT3-L (50 ng/mL), TPO (50 ng/mL), and IL-3 (10 ng/mL) for 24 hours. Cells were then transduced with Lenti/iNKT-sr39TK for 24 hours. To generate ^{Allo}HSC-iNKT cells, non-tissue culture-treated 24-well plates were coated with StemSpan lymphoid differentiation coating material (LDCM, 500μl/well, StemCell Technologies, Vancouver, Canada) for 2 hours at room temperature. Transduced CD34$^+$ HSCs were then suspended in StemSpan lymphoid progenitor expansion medium (LPEM, StemCell Technologies) and seeded into coated wells of the 24-well plate on day 0. The cells were then cultured for 4 days before an additional 500 μL of LPEM medium was added to each well. Half of the medium was removed and replenished every 3-4 days. On day 14, cells were harvested, counted, and reseeded into an LDCM-coated 12-well plate in 1 mL of T cell progenitor maturation medium per well (TPMM, StemCell Technologies) (5 x 10^5 - 1 x 10^6 cells/well). On day 18, 1 mL of fresh TPMM was added to each well. Half of the medium was removed and replenished with 1mL of TPMM every 3-4 days. On day 28, cells were harvested, counted, and re-seeded into a new coated 12-well plate in 1 mL of TPMM (1 x 10^6 cells/mL/well) with 12.5 μL/well CD3/CD28/CD2 T Cell Activator (StemCell Technologies) and 10 ng/mL human recombinant IL-15 (PeproTech). On Day 31, 1 mL of fresh TPMM containing 10 ng/mL human recombinant IL-15 was added into the culture. On day 35, cells were harvested and analyzed by flow cytometry. The generated ^{Allo}HSC-iNKT cells were then expanded using αGC/PBMCs, in which healthy donor PBMCs were loaded with α-Galactosylceramide (αGC) and irradiated at 6,000 rads. Freshly generated

^{Allo}HSC-iNKT cells were mixed with αGC/PBMCs and cultured in C10 medium with IL-7 and IL-15. ^{Allo}HSC-iNKT cells were allowed to expand for 7-14 days, then were aliquoted and frozen in liquid nitrogen storage tanks for future use. All cultures described here were carried out in OpTmizer™ CTS™ T-Cell Expansion serum-free medium (Gibco, Thermo Fisher Scientific).

In vitro generation of healthy donor PBMC-Derived conventional αβ T (PBMC-T) cells

Healthy donor-derived PBMCs were provided by the UCLA/CFAR Virology Core Laboratory, without identification information under federal and state regulations. These PBMCs were stimulated with CD3/CD28 T-activator beads (ThermoFisher Scientific) and cultured in C10 medium supplemented with human IL-2 (20 ng/mL) for 2–3 weeks to generate PBMC-T cells, following the manufacturer's instructions.

In vitro generation of healthy donor PBMC-Derived NK (PBMC-NK) cells

Healthy donor PBMCs were FACS-sorted via human CD56 antibody (Clone HCD56; Biolegend) labeling or MACS- sorted using a human NK Cell Isolation Kit (Miltenyi Biotech). Freshly sorted PBMC-NK cells were used to the *in vitro* tumor cell killing assays.

In vitro generation of mesothelin-targeting chimeric antigen receptor-engineered conventional αβ T (MCAR-T) cells

Healthy donor PBMCs were stimulated with CD3/CD28 T-activator beads (ThermoFisher Scientific) in the presence of recombinant human IL-2 (30 ng/ml), following the manufacturer's instructions. 2 days after activation of the PBMC cultures, cells were washed, resuspended in the fresh C10 medium, and then concentrated Lenti/MCAR viruses were added to the PBMC cultures. The following day, transduced cells were washed and passaged 3 times per week for 2 weeks to maintain a cell density at 0.5∼1 x 10^6 cells/mL; fresh C10 medium was added at every passage. The resulting MCAR-T cells were collected and cryopreserved for future use.

In vitro generation of NY-ESO-1-targeting TCR-Engineered conventional αβ T (ESO-T) cells

Healthy donor PBMCs were stimulated with CD3/CD28 T-activator beads (ThermoFisher Scientific) in the presence of recombinant human IL-2 (30 ng/ml), following the manufacturer's instructions. 2 days after activation of the PBMC cultures, cells were washed, resuspended in the fresh C10 medium, and then concentrated Lenti/1G4-TK viruses were added to the PBMC cultures. The following day, transduced cells were washed and passaged 3 times per week for 2 weeks to maintain a cell density at 0.5∼1 x 10^6 cells/mL; fresh C10 medium was added at every passage. The resulting ESO-T cells were collected and cryopreserved for future use.

Profiling tumor cells of primary OC patient samples using flow cytometry

Phenotypes of live tumor cells (gated as e506$^-$CD45$^-$FAP$^-$CD31$^-$) from recurrent and chemonaive OC patient samples were analyzed using flow cytometry. Cell surface markers and transcription factors including CAR antigens (MSLN and MUC16), ESO TCR antigen (NY-ESO-1), NK dligands (ULBP-1, ULBP-2/5/6, MICA/B, CD112, and CD155), HLA molecules (HLA-I, and HLA-II), Cancer Stem Cell (CSC) surface markers (CD24, CD44, CD117, and CD133), and CSC transcription factors (Oct3/4, SOX2, and Nanog) were utilized to study tumor cell phenotype of primary OC patient samples.

Profiling tumor microenvironment (TME) of primary OC patient samples using flow cytometry

Composition of live immune cells (gated as e506$^-$CD45$^+$) from recurrent and chemonaive OC patient samples were analyzed using flow cytometry. Cell surface markers including human CD1d, T cell markers (TCR αβ, CD4 and CD8), B cell marker (CD19), NK cell marker (CD56), and macrophage markers (CD11b, CD14, CD86, CD206, HLA-DR, and CD163) were utilized to study immune cell composition and phenotype of primary OC patient samples.

In vitro primary OC patient sample-derived tumor cell killing assay

To study the OC patient sample-derived tumor cell killing capacity of therapeutic cells, the samples were first sorted using a human tumor cell isolation kit (Miltenyi Biotec, CAT #130-108-339) to deplete CD45$^+$ immune cells, CD31$^+$ endothelial cells, and FAP$^+$ fibroblast cells following the manufacturer's instructions. Primary OC patient sample-derived tumor cells were then co-cultured with MCAR-T cells (tumor:MCAR-T ratio 1:1), ESO-T cells (tumor:ESO-T ratio 1:2), NK cells (tumor:NK ratio 1:5), or ^{Allo}HSC-iNKT cells (tumor:iNKT ratio 1:2) in 96-well round bottom plates in C10 medium for 24 hours. After the culture, cells were collected to quantify live tumor cells using flow cytometry. Healthy donor PBMC-derived T and B cells were included as safety controls to study the killing capacity of ^{Allo}HSC-iNKT cells. In some experiments, 10 μg/ml of LEAF™ purified anti-human NKG2D (Clone 1D11, Biolegend), anti-human DNAM-1 antibody (Clone 11A8, Biolegend), or LEAF™ purified mouse IgG2bk isotype control antibody (Clone MG2B-57, Biolegend) was added to co-cultures, to study NK activating receptor-mediated tumor cell killing mechanism.

In vitro primary OC patient sample-derived immune cell killing assay

Chemonaive and recurrent OC patient samples were co-cultured with PBMC-T cells or ^{Allo}HSC-iNKT cells (ratio 1:1) in C10 medium in Corning 96-well Round Bottom Cell Culture plates for 24 hours. After 24 hours, cells were collected and ^{Allo}HSC-iNKT cell killing efficacy was assessed using flow cytometry by detecting live TAMs/MDSCs (gated as CD11b$^+$), T cells (gated as CD3$^+$), B cells (gated as CD19$^+$) and NK cells (gated

as CD56^{+}). To study the immune composition of OC patient sample-derived cells co-cultured with ^{Allo}HSC-iNKT cells, iNKT TCR^{-} (6B11^{-}) cells were pre-gated to separate ^{Allo}HSC-iNKT cells and patient-derived cells. To study the immune composition of OC patient sample-derived cells co-cultured with PBMC-T cells, a pair of HLA-A2^{+} patient-derived cells and HLA-A2^{-} PBMC-T cells, or a pair of HLA-A2^{-} patient-derived cells and HLA-A2^{+} PBMC-T cells were used to set up the assay; HLA-A2 was used to separate PBMC-T cells and patient-derived cells. In some assays, 10 μg/ml LEAF™ purified anti-human CD1d antibody (Clone 51.1, Biolegend) or LEAF™ purified mouse IgG2b k isotype control antibody (Clone MG2b-57, Biolegend) was added to TAM/MDSC culture one hour prior to adding ^{Allo}HSC-iNKT cells.

In vitro healthy donor-derived immune cell killing assay

Healthy donor PBMCs were co-cultured with ^{Allo}HSC-iNKT cells (ratio 1:1) in C10 medium in Corning 96-well Round Bottom Cell Culture plates for 24 hours. After 24 hours, cells were collected and ^{Allo}HSC-iNKT cell killing efficacy was assessed using flow cytometry by detecting live T cells (gated as CD3^{+}iNKT TCR^{-}) and B cells (gated as CD19^{+}).

QUANTIFICATION AND STATISTICAL ANALYSIS

A Prism 8 software (Graphpad) was utilized for all statistical analysis. Pairwise comparisons were performed with a 2-tailed Student's t test. Multiple comparisons were performed with an ordinary 1-way ANOVA, followed by Tukey's multiple comparisons test. Unless otherwise indicated, data are presented as the mean ± SEM. In all figures and figure legends, "n" represents the number of biological replicates in which the experiment was performed. A P value of less than 0.05 was considered significant. ns, not significant; *$p < 0.05$; **$p < 0.01$; ***$p < 0.001$; ****$p < 0.0001$.

iScience, Volume *26*

Supplemental information

Profiling ovarian cancer tumor and microenvironment during disease progression for cell-based immunotherapy design

Yan-Ruide Li, Christopher J. Ochoa, Yichen Zhu, Adam Kramer, Matthew Wilson, Ying Fang, Yuning Chen, Tanya Singh, Gabriella Di Bernardo, Enbo Zhu, Derek Lee, Neda A. Moatamed, Joanne Bando, Jin J. Zhou, Sanaz Memarzadeh, and Lili Yang

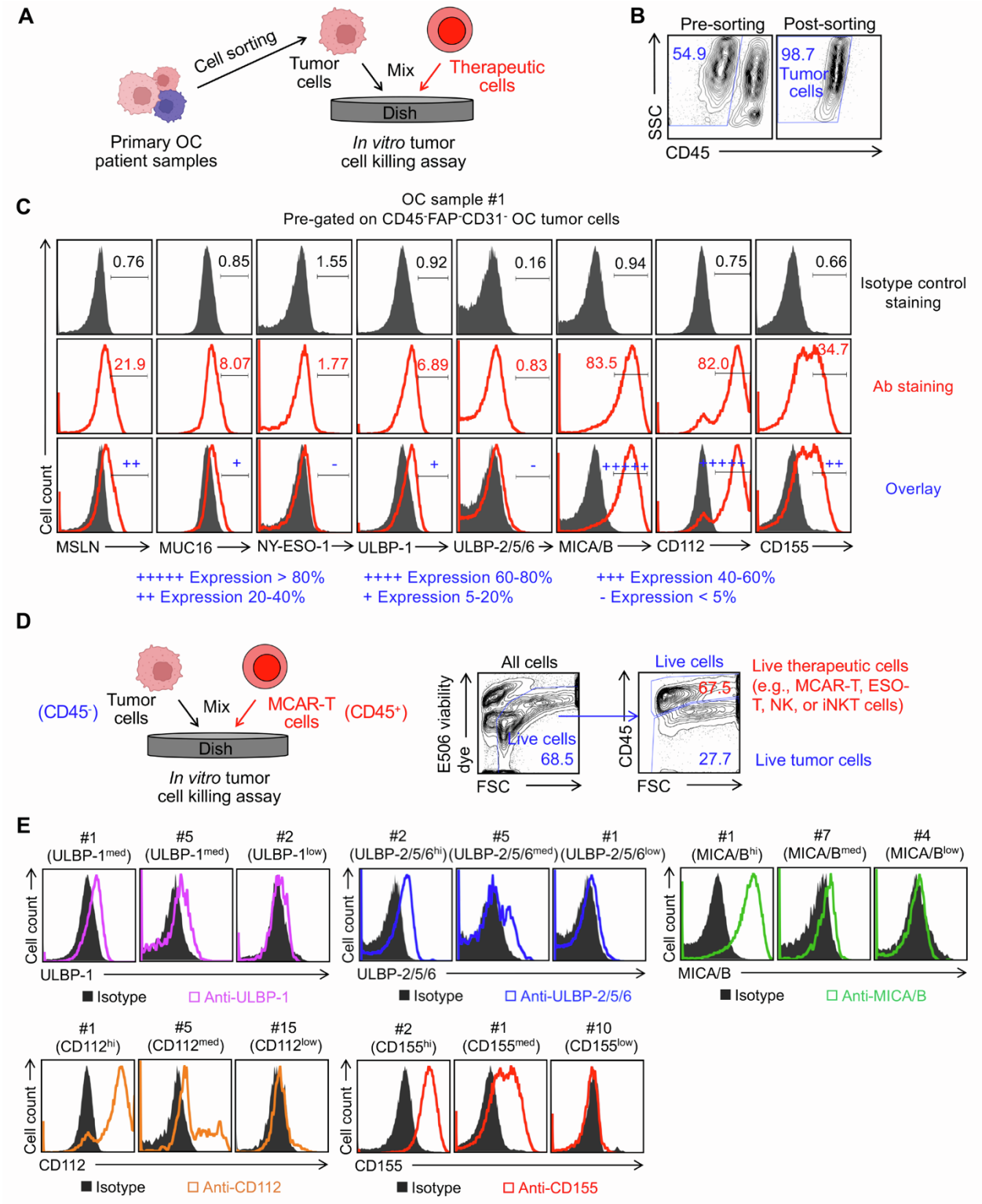

Figure S1. OC tumor cell killing assay; related to Figure 1.

(A) The process of sorting tumor cells from OC samples and conducting an *in vitro* assay to assess tumor cell killing by various therapeutic cells.

(B) FACS detection of tumor cells before and after tumor cell sorting.

(C) Flow gating strategy to detect antigen expression on OC tumor cells. OC sample #1 was presented as an example.
(D) Flow gating strategy to detect live tumor cells and therapeutic cells in the *in vitro* primary OC patient sample-derived tumor cell killing assay. The killing by MCAR-T cells was presented as an example.
(E) FACS analyses of NK ligand expression on tumor cells from OC patient samples. NK ligand high, medium, and low-expressing tumor samples were presented.

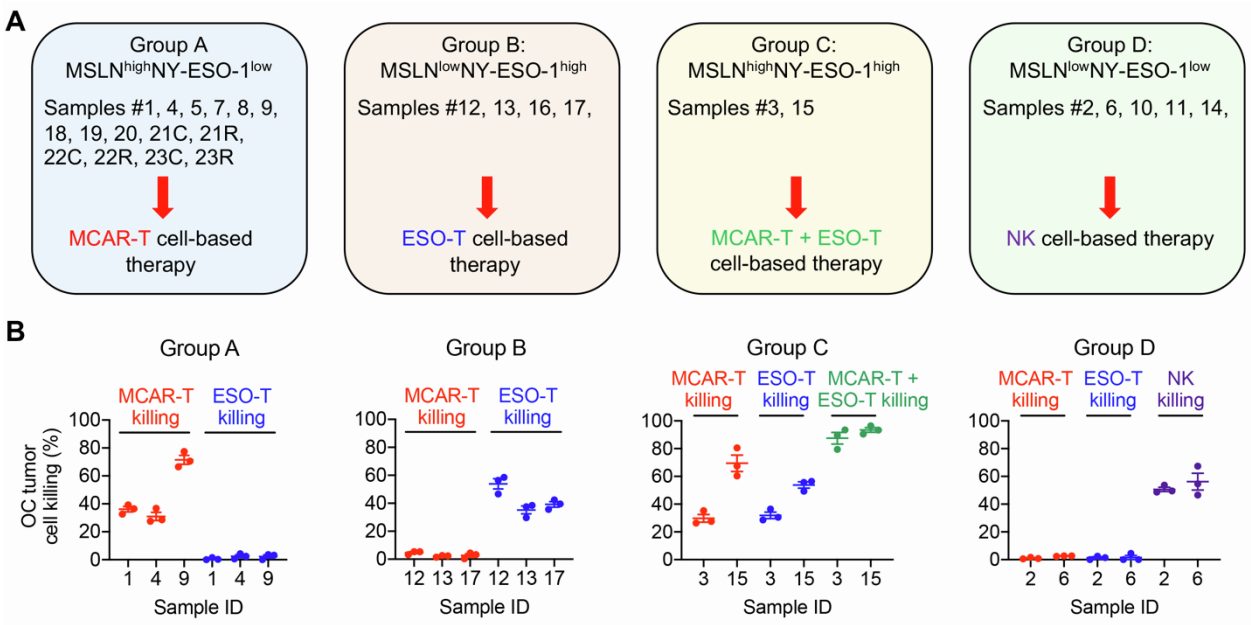

Figure S2. A stratification strategy to optimize CBIs based on OC tumor characteristics; related to Figure 1.

(A) Classification of OC samples based on the expression levels of MSLN and NY-ESO-1.

(B) OC tumor cell killing data by the indicated therapeutic cells at 24 h (n = 3). MCAR-T:tumor = 1:1, ESO-T:tumor = 2:1, NK:tumor = 5:1. For group C, the same healthy donor-derived MCAR-T and ESO-T cells were mixed, and then co-cultured with OC tumor cells to study their synergetic tumor cell killing efficacy, MCAR-T:ESO-T:tumor = 1:2:1.

Representative of 1 experiment. Data are presented as the mean ± SEM.

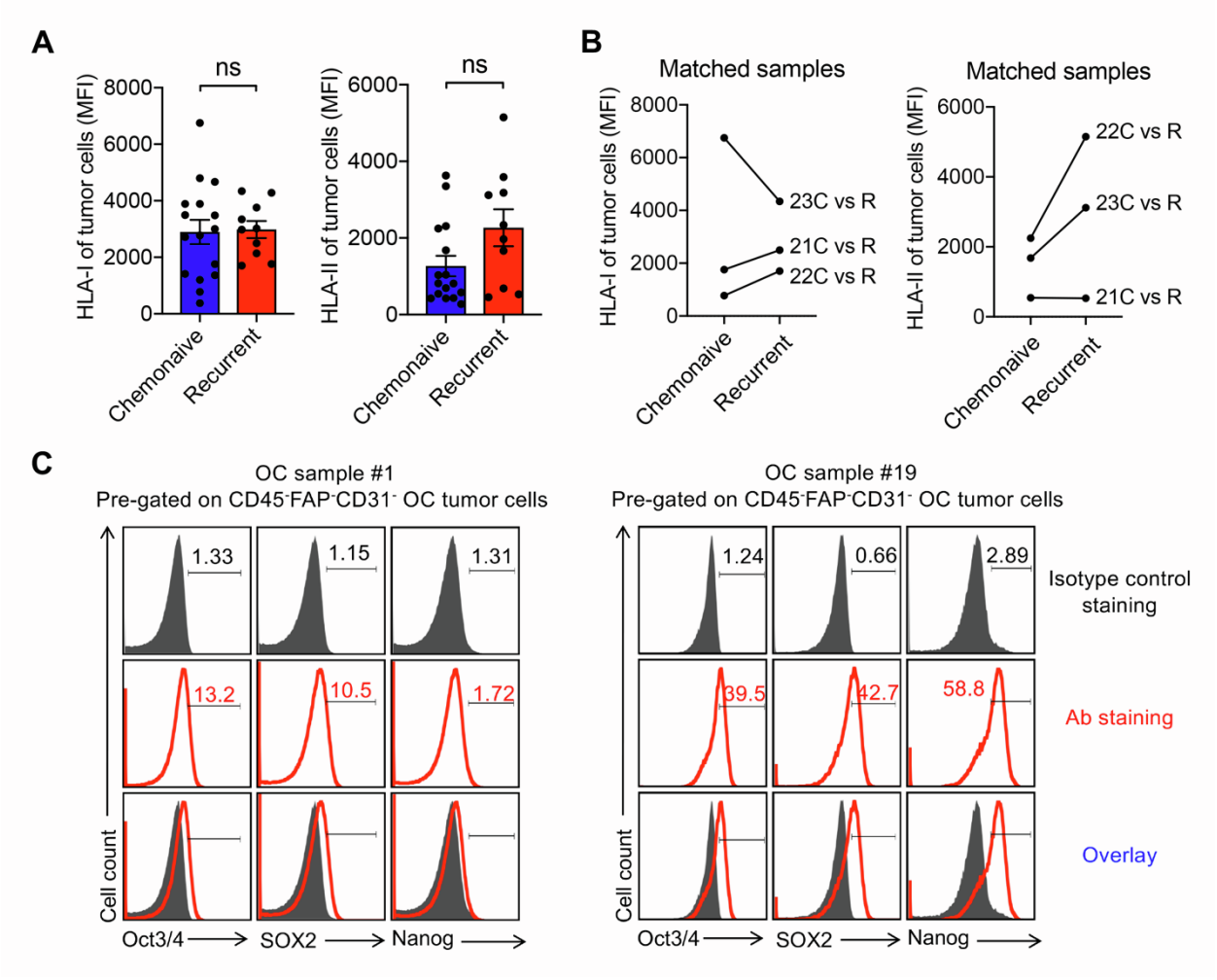

Figure S3. HLA molecule expression on OC tumor cells, and CSC transcription factor gating strategy; related to Figure 1.

(A) Quantification of HLA-I and HLA-II expression on tumor cells between chemonaive and recurrent samples.

(B) HLA expression on tumor cells from 3 matched patient samples.

(C) Flow gating strategy to detect CSC transcription factor (CSC-TF) expression in OC tumor cells. OC sample #1 (CSC-TF low) and #19 (CSC-TF high) were presented as an example.

Representative of 1 (A and B) and > 20 (C) experiments. Data are presented as the mean ± SEM. ns, not significant, by Student's *t* test.

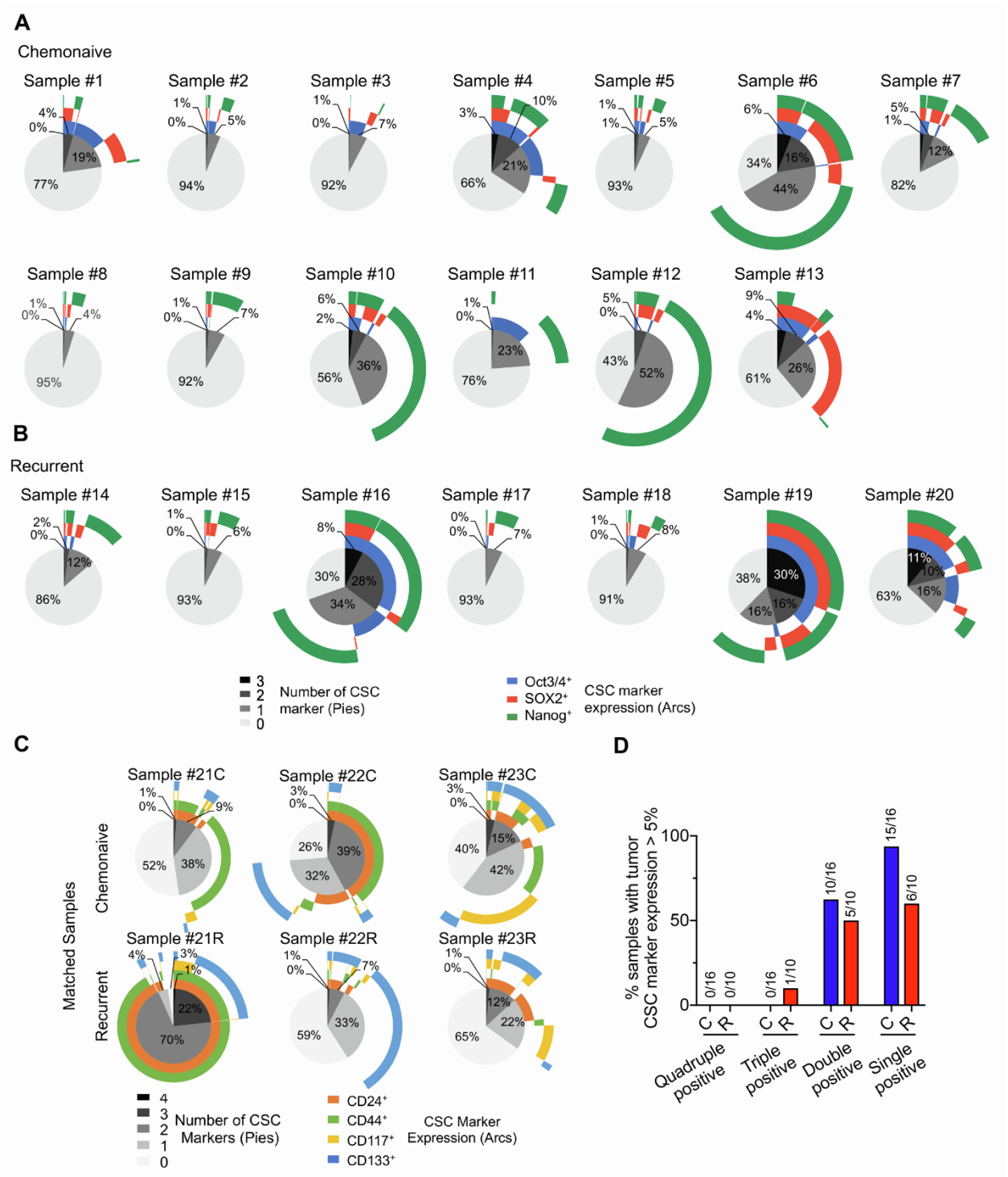

Figure S4. CSC feature of OC tumor cells; related to Figure 1.

(A-B) SPICE analysis of CSC transcription factor expression on tumor cells. Pie charts reflect proportions of indicated tumor cell groups expressing indicated numbers (0–3) of CSC transcription factors. Colored arcs indicate the specific combinations of CSC markers expressed. Data from chemonaive (A) and recurrent (B) patient samples were presented.

(C) SPICE analysis of CSC surface marker expression on tumor cells. CD24, CD44, CD117, and CD133 were used as surface markers.
(D) Summary of OC patient samples categorized based on the expression level of CSC surface markers.
Representative of 1 experiment.

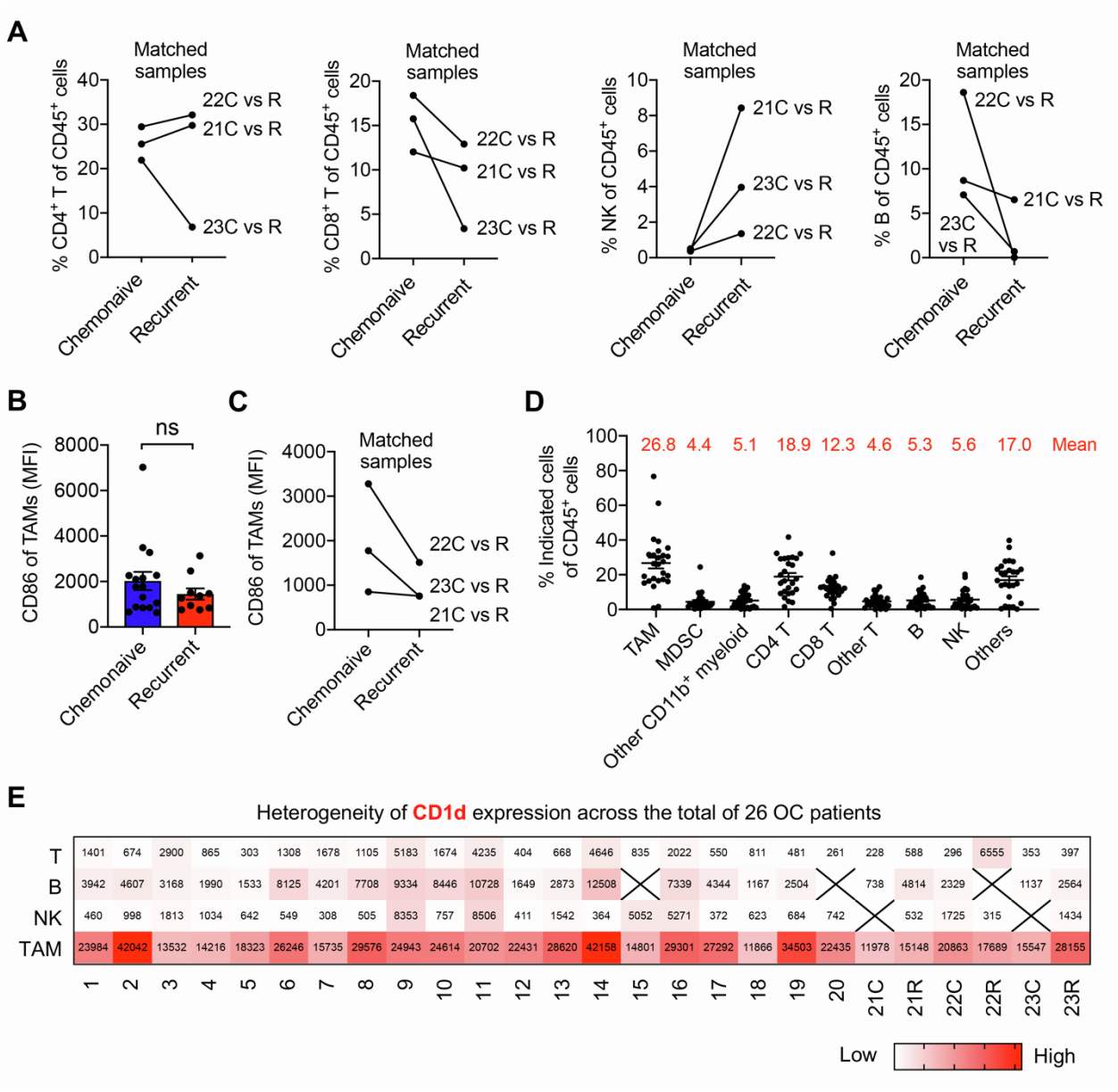

Figure S5. OC TME immune cell composition; related to Figure 2.

(A) Quantification of CD4$^+$ T, CD8$^+$ T, B, and NK cell percentage of CD45$^+$ immune cells in the 3 matched patient samples before and after chemotherapy.

(B-C) Quantification of CD86 expression on TAMs between chemonaive and recurrent samples. Total 26 OC samples (B) and 3 paired of matched samples (C) were shown.

(D) Summary of the percentage of indicated cells among CD45$^+$ immune cells, along with the mean values of these percentages.

(E) A heatmap illustrating the heterogeneity of CD1d expression across the total of 26 OC patients is presented. The mean fluorescence intensity (MFI) values of CD1d on the indicated cells are depicted. Cells with low cell numbers are excluded from the CD1d data representation.

Data are presented as the mean ± SEM. ns, not significant, by Student's *t* test.

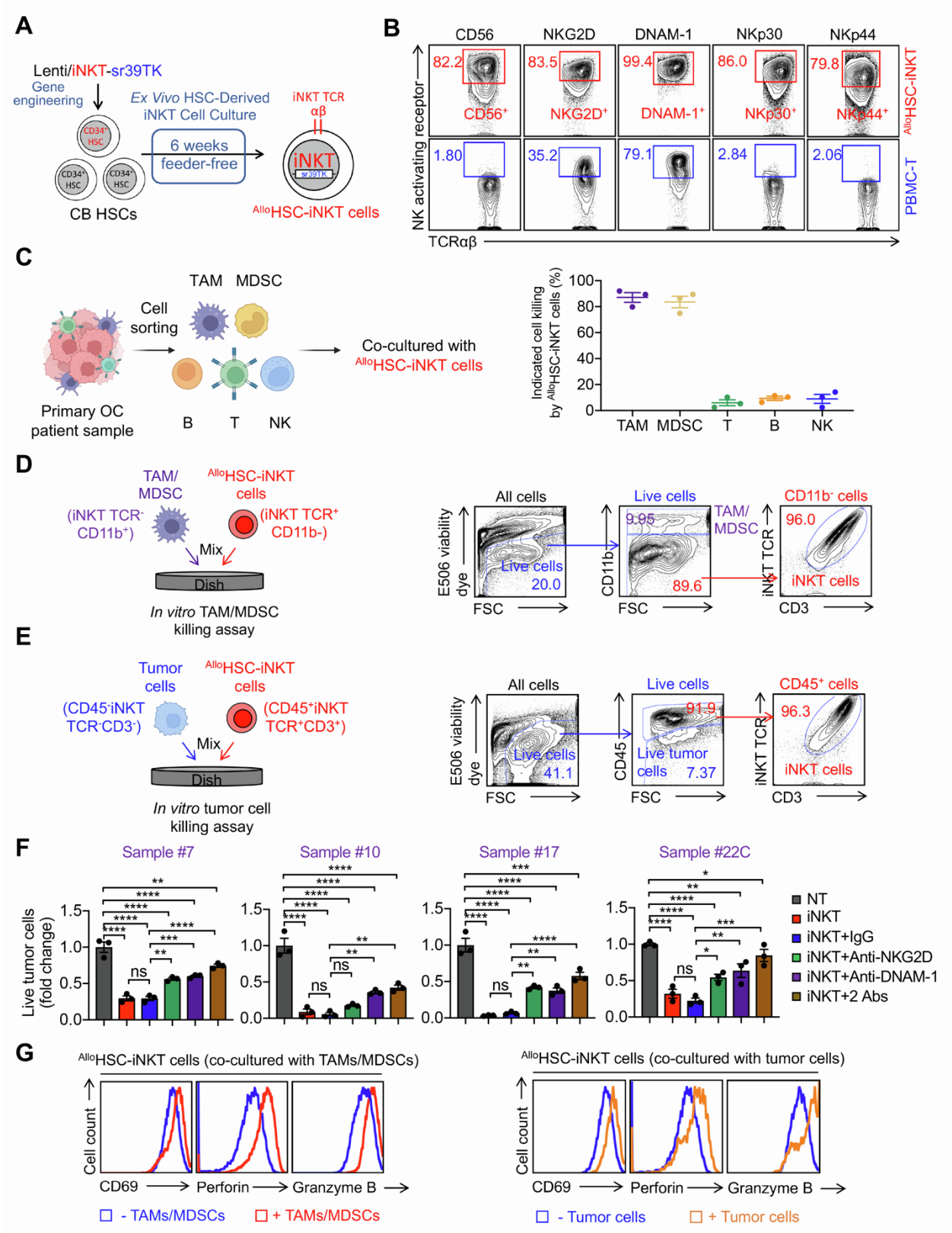

Figure S6. Generation and characterization of allogeneic HSC-derived iNKT (^{Allo}HSC-iNKT) cells; related to Figure 3.

(A) Diagram showing the generation of ^{Allo}HSC-iNKT cells. CB, cord blood.
(B) FACS detection of surface NK activating receptors on ^{Allo}HSC-iNKT cells. Conventional PBMC-derived T (PBMC-T) cells were included as a control.
(C) TAM, MDSC, T, B, and NK cell killing data by ^{Allo}HSC-iNKT cells at 24 h (n = 3). In certain experiments, we employed cell sorting to isolate specific cell populations, which were then co-cultured directly with ^{Allo}HSC-iNKT cells. This approach minimized potential interactions between different immune cells, ensuring a focused assessment of the killing outcomes. Thus, the observed cytotoxic effects of ^{Allo}HSC-iNKT cells on the targeted TAMs and MDSCs are attributed solely to their direct interactions.
(D) Flow gating strategy to identify live TAMs or MDSCs and ^{Allo}HSC-iNKT cells in the *in vitro* TAM/MDSC killing assay.
(E) Flow gating strategy to identify live tumor and ^{Allo}HSC-iNKT cells in the *in vitro* tumor cell killing assay.
(F) Studying the tumor cell killing efficacy and mechanisms of ^{Allo}HSC-iNKT cells. Tumor cell killing data at 24 h (E:T = 2:1, n = 3). Anti-NKG2D and/or anti-DNAM-1 antibodies were added into the coculture to block NK receptor/ligand recognition.
(G) FACS analyses of activation marker CD69 and cytotoxic molecules Perforin and Granzyme B of ^{Allo}HSC-iNKT cells 24 hours after coculturing with TAMs/MDSCs or OC tumor cells (n = 3).
Representative of 3 (A-C, and G), and > 20 (D-F) experiments. Data are presented as the mean ± SEM. ns, not significant, *p < 0.05, **p < 0.01, ***p < 0.001, ****p < 0.0001, by one-way ANOVA.

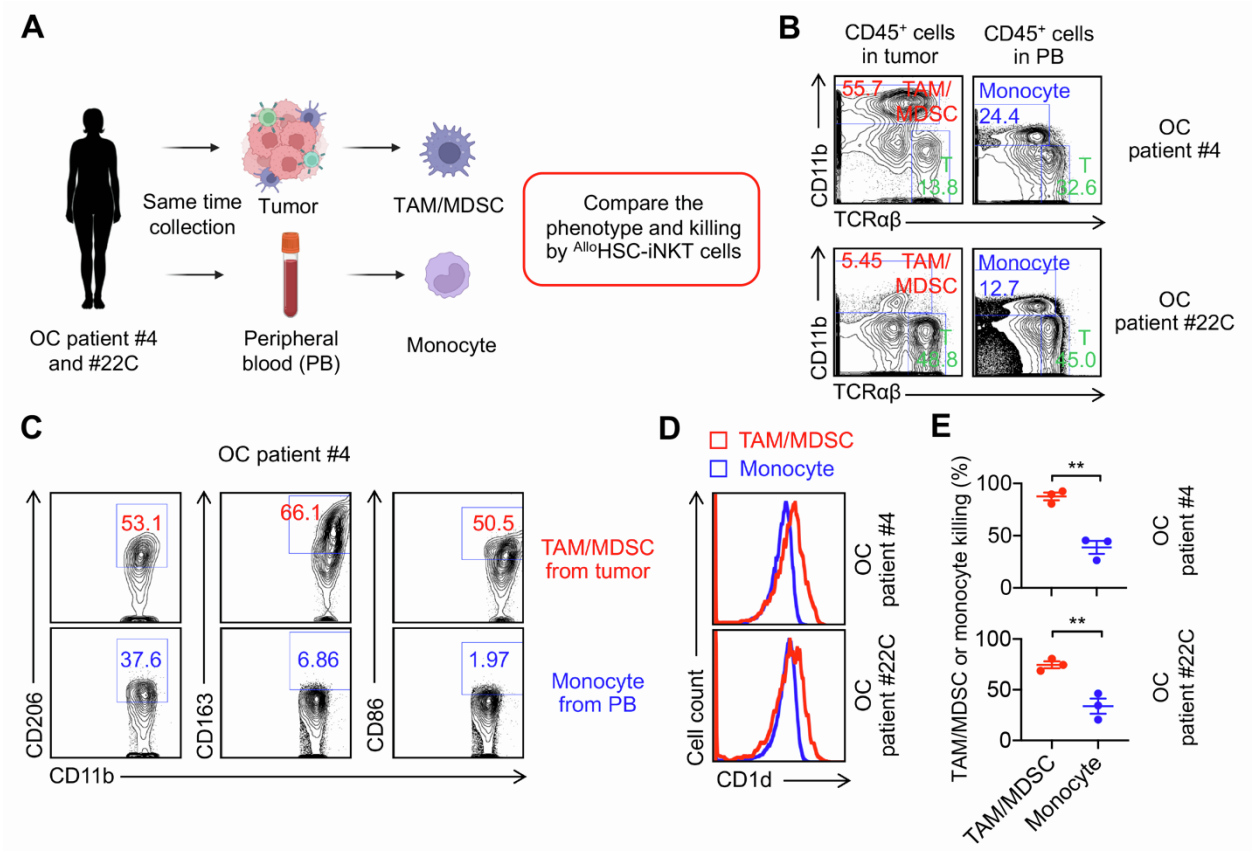

Figure S7. Comparison of PBMC monocytes and TAMs/MDSCs from the tumor site in the same OC patients; related to Figure 3.

(A) Experimental design to collect and study PBMC monocytes and TAMs/MDSCs from the tumor site in the same OC patient. Data from OC patient #4 and #22C were presented.

(B) Flow cytometry showing the TAMs/MDSCs and monocytes.

(C) FACS detection of CD163, CD206, and CD86 on TAMs/MDSCs and monocytes. Data from patient #4 were presented.

(D) FACS detection of CD1d on TAMs/MDSCs and monocytes.

(E) TAM/MDSC and monocyte killing data by ^{Allo}HSC-iNKT cells at 24 h (n = 3).

Representative of 2 experiments. Data are presented as the mean ± SEM. **$p < 0.01$, by Student's *t* test.